Fiber Orientation ~~and Length~~ Modeling: The Concepts Behind the Calculations

Charles Tucker

Department of Mechanical Science and Engineering, University of Illinois at Urbana-Champaign

Processing controls properties by affecting fiber orientation, so we want to predict orientation

Processing

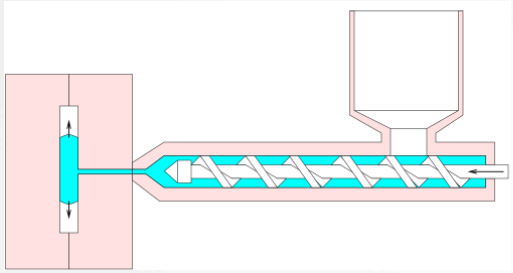

Properties

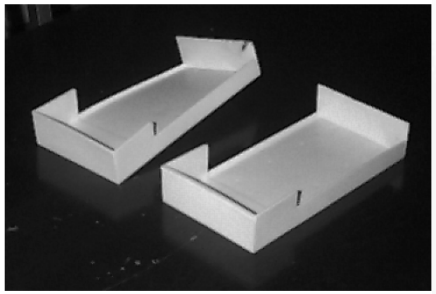

microstructure prediction

Structure

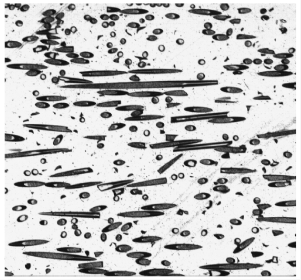

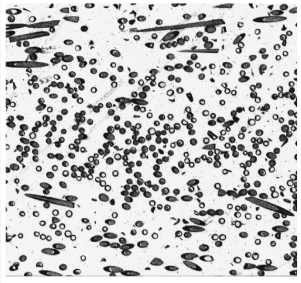

micromechanics modeling

Key learning objectives

At the end of this class, you will be able to:

- Identify and apply the two qualitative rules of flow-induced fiber orientation
- Explain how fiber orientation is represented and calculated within Autodesk Moldflow
- Describe the ideas behind different fiber orientation models (Folgar-Tucker, RSC, ARD)
- Explain how material parameters in these models are determined from experimental data

The broad outline:

- Where fiber orientation modeling began (Jeffery's equation)
- Qualitative rules and fiber orientation phenomena
- The problems with Jeffery model, and their solutions (Folgar-Tucker, orientation tensors, RSC, ARD)
- Advice on modeling options and setting model parameters

It all started with Einstein

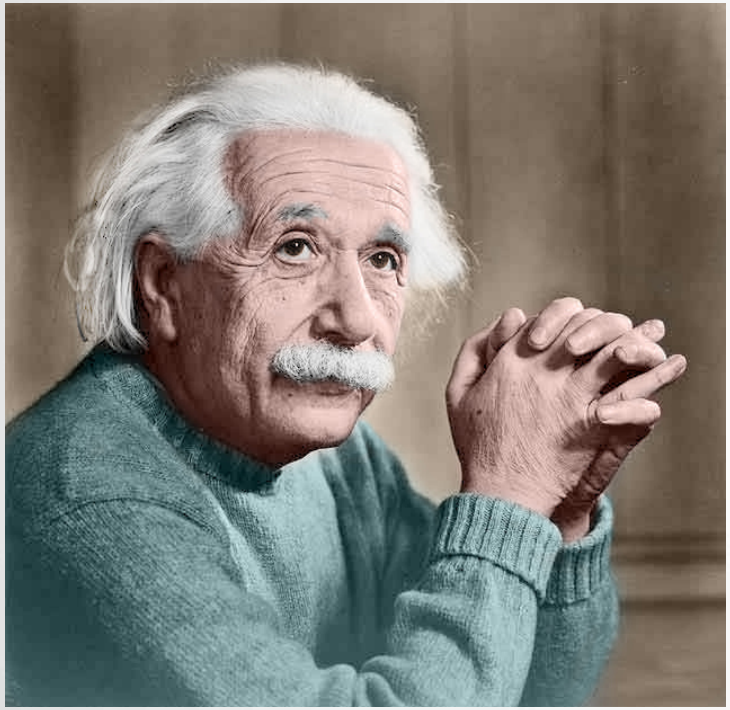

- Predicted the viscosity increase by adding spherical particles to a Newtonian fluid (1911):

$$\mu = \mu_0 + 2.5\varphi$$

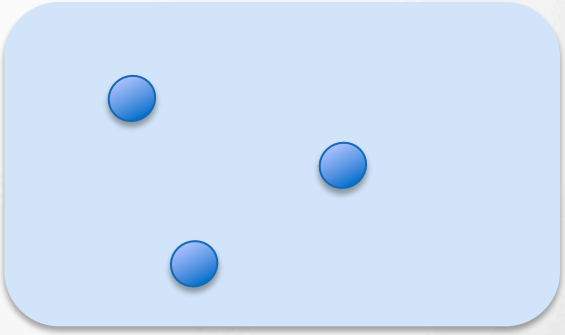

Jeffery is the father of fiber orientation

- George Barker Jeffery, 1891-1957
- Fellow of the Royal Society
- Professor of Mathematics, University College, London
- “We have extended [Einstein’s] work to the case of particles of ellipsoidal shape.”

E. C. Titchmarsh, *Biographical Memoirs of Fellows of the Royal Society*, Vol. 4 (Nov., 1958), pp. 128-137

Jeffery's greatest hit (1922)

The Motion of Ellipsoidal Particles Immersed in a Viscous Fluid.

By G. B. JEFFERY, M.A., D.Sc., Fellow of University College, London.

(Communicated by Prof. L. N. G. Filon, F.R.S. Received January 30, 1922.)

§ 1. *Introduction.*

In both physical and biological science, we are often concerned with the properties of a fluid, or plasma, in which small particles or corpuscles are suspended and carried about by the motion of the fluid. The presence of the particles will influence the properties of the suspension in bulk, and, in particular, its viscosity will be increased. The most complete mathematical treatment of the problem, from this point of view, has been that given by Einstein,* who considered the case of spherical particles and gave a simple formula for the increase in the viscosity. We have extended this work to the case of particles of ellipsoidal shape.

The second section of the paper is occupied with the requisite solution of the equations of motion of the fluid. The problem of the motion of a viscous fluid, due to an ellipsoid moving through it with a small velocity of translation in a direction parallel to one of its axes, has been solved by Oberbeck,† and the corresponding problem for an ellipsoid rotating about one of its axes by Edwards.‡ In both cases the equations of motion are approximated by neglecting the terms involving the squares of the velocities. It may be seen,

* "Eine neue Bestimmung der Moleküldimensionen," 'Ann. d. Physik,' vol. 19, p. 289 (1896); with a correction in vol. 34, p. 591 (1911).

† 'Crelle,' vol. 81 (1876).

‡ 'Quart. Jour. Math.,' vol. 26 (1892).

From (7) we have

$$\frac{\partial\lambda}{\partial x}=\frac{2x\mathrm{P}^2}{a^2+\lambda},\quad \frac{\partial\lambda}{\partial y}=\frac{2y\mathrm{P}^2}{b^2+\lambda},\quad \frac{\partial\lambda}{\partial z}=\frac{2z\mathrm{P}^2}{c^2+\lambda} \tag{14}$$

where

$$\frac{1}{\mathrm{P}^2}=\frac{x^2}{(a^2+\lambda)^2}+\frac{y^2}{(b^2+\lambda)^2}+\frac{z^2}{(c^2+\lambda)^2}. \tag{15}$$

We then have a number of formulæ of which the following are typical:

$$\frac{\partial\Omega}{\partial x}=2\alpha x,\quad \frac{\partial^2\Omega}{\partial x^2}=2\alpha-\frac{4x^2\mathrm{P}^2}{(a^2+\lambda)^2\Delta},\quad \frac{\partial^2\Omega}{\partial y\,\partial z}=-\frac{4yz\mathrm{P}^2}{(b^2+\lambda)(c^2+\lambda)\Delta}, \tag{16}$$

and

$$\frac{\partial\chi_1}{\partial x}=\frac{\partial\chi_2}{\partial y}=\frac{\partial\chi_3}{\partial z}=-\frac{2xyz\mathrm{P}^2}{\Delta^2},$$

$$\frac{\partial\chi_1}{\partial y}=\alpha' z-\frac{2y^2z\mathrm{P}^2}{(b^2+\lambda)^2(c^2+\lambda)\Delta},\quad \frac{\partial\chi_1}{\partial z}=\alpha' y-\frac{2yz^2\mathrm{P}^2}{(b^2+\lambda)(c^2+\lambda)^2\Delta}. \tag{17}$$

All these differential coefficients tend to zero at infinity.

We assume

$$\begin{aligned}u=u_0&+\frac{\partial}{\partial x}(\mathrm{R}\chi_1+\mathrm{S}\chi_2+\mathrm{T}\chi_3)+\mathrm{W}\frac{\partial\chi_3}{\partial y}-\mathrm{V}\frac{\partial\chi_2}{\partial z}\\&+\mathrm{A}\left(x\frac{\partial^2\Omega}{\partial x^2}-\frac{\partial\Omega}{\partial x}\right)+\mathrm{H}\left(x\frac{\partial^2\Omega}{\partial x\,\partial y}-\frac{\partial\Omega}{\partial y}\right)+\mathrm{G}'\left(x\frac{\partial^2\Omega}{\partial x\,\partial z}-\frac{\partial\Omega}{\partial z}\right)\\&+y\left(\mathrm{H}'\frac{\partial^2\Omega}{\partial x^2}+\mathrm{B}\frac{\partial^2\Omega}{\partial x\,\partial y}+\mathrm{F}\frac{\partial^2\Omega}{\partial x\,\partial z}\right)\\&+z\left(\mathrm{G}\frac{\partial^2\Omega}{\partial x^2}+\mathrm{F}'\frac{\partial^2\Omega}{\partial x\,\partial y}+\mathrm{C}\frac{\partial^2\Omega}{\partial x\,\partial z}\right),\end{aligned} \tag{18}$$

$$\begin{aligned}v=v_0&+\frac{\partial}{\partial y}(\mathrm{R}\chi_1+\mathrm{S}\chi_2+\mathrm{T}\chi_3)+\mathrm{U}\frac{\partial\chi_1}{\partial z}-\mathrm{W}\frac{\partial\chi_3}{\partial x}\\&+x\left(\mathrm{A}\frac{\partial^2\Omega}{\partial x\,\partial y}+\mathrm{H}\frac{\partial^2\Omega}{\partial y^2}+\mathrm{G}'\frac{\partial^2\Omega}{\partial y\,\partial z}\right)\\&+\mathrm{H}'\left(y\frac{\partial^2\Omega}{\partial x\,\partial y}-\frac{\partial\Omega}{\partial x}\right)+\mathrm{B}\left(y\frac{\partial^2\Omega}{\partial y^2}-\frac{\partial\Omega}{\partial y}\right)+\mathrm{F}\left(y\frac{\partial^2\Omega}{\partial y\,\partial z}-\frac{\partial\Omega}{\partial z}\right)\\&+z\left(\mathrm{G}\frac{\partial^2\Omega}{\partial x\,\partial y}+\mathrm{F}'\frac{\partial^2\Omega}{\partial y^2}+\mathrm{C}\frac{\partial^2\Omega}{\partial y\,\partial z}\right),\end{aligned} \tag{19}$$

and

$$\begin{aligned}w=w_0&+\frac{\partial}{\partial z}(\mathrm{R}\chi_1+\mathrm{S}\chi_2+\mathrm{T}\chi_3)+\mathrm{V}\frac{\partial\chi_2}{\partial x}-\mathrm{U}\frac{\partial\chi_1}{\partial y}\\&+x\left(\mathrm{A}\frac{\partial^2\Omega}{\partial x\,\partial z}+\mathrm{H}\frac{\partial^2\Omega}{\partial y\,\partial z}+\mathrm{G}'\frac{\partial^2\Omega}{\partial z^2}\right)\\&+y\left(\mathrm{H}'\frac{\partial^2\Omega}{\partial x\,\partial z}+\mathrm{B}\frac{\partial^2\Omega}{\partial y\,\partial z}+\mathrm{F}\frac{\partial_2\Omega}{\partial z^2}\right)\\&+\mathrm{G}\left(z\frac{\partial^2\Omega}{\partial x\,\partial z}-\frac{\partial\Omega}{\partial x}\right)+\mathrm{F}'\left(z\frac{\partial^2\Omega}{\partial y\partial z}-\frac{\partial\Omega}{\partial y}\right)+\mathrm{C}\left(z\frac{\partial^2\Omega}{\partial z^2}-\frac{\partial\Omega}{\partial z}\right).\end{aligned} \tag{20}$$

Jeffery analyzed a single, ellipsoidal particle

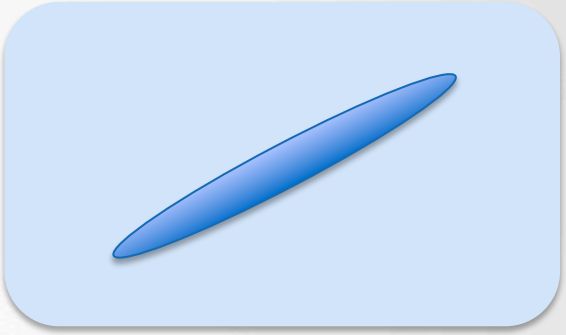

Assuming:

- Newtonian fluid
- Linear velocity field far away from the particle
- Negligible buoyancy and inertia

An exact, closed-form solution!

Then:

- No external force on the particle → the particle moves with the fluid
- No external torque on the particle → the particle rotates according to Jeffery's equation

Jeffery's equation gives us two rules for fiber orientation:

Shearing flows: fibers align in the shearing direction

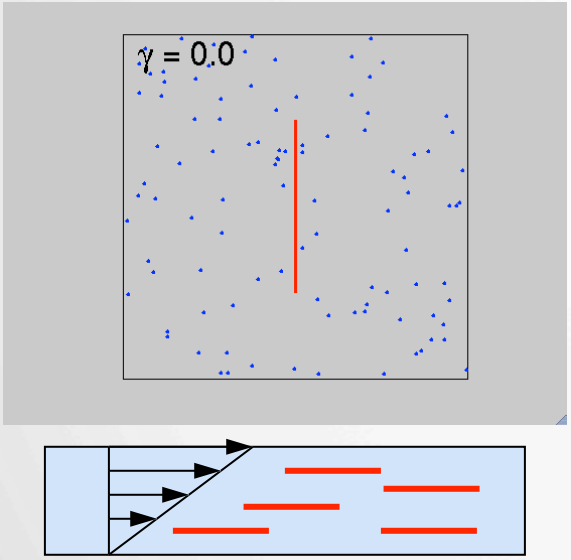

Stretching flows: fibers align in the stretching direction

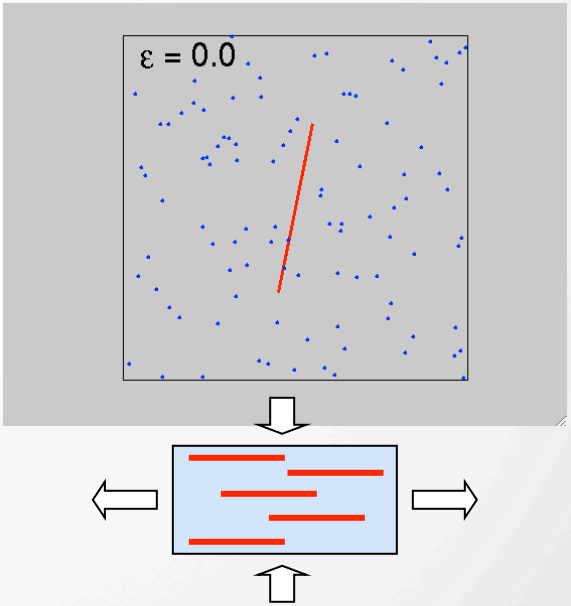

These two rules explain **all** fiber orientation phenomena in injection molding

Shearing flows: fibers align in the shearing direction

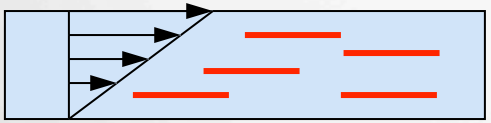

Stretching flows: fibers align in the stretching direction

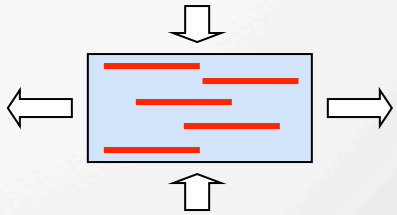

Example 1: All parts have a shell layer highly aligned in the flow direction

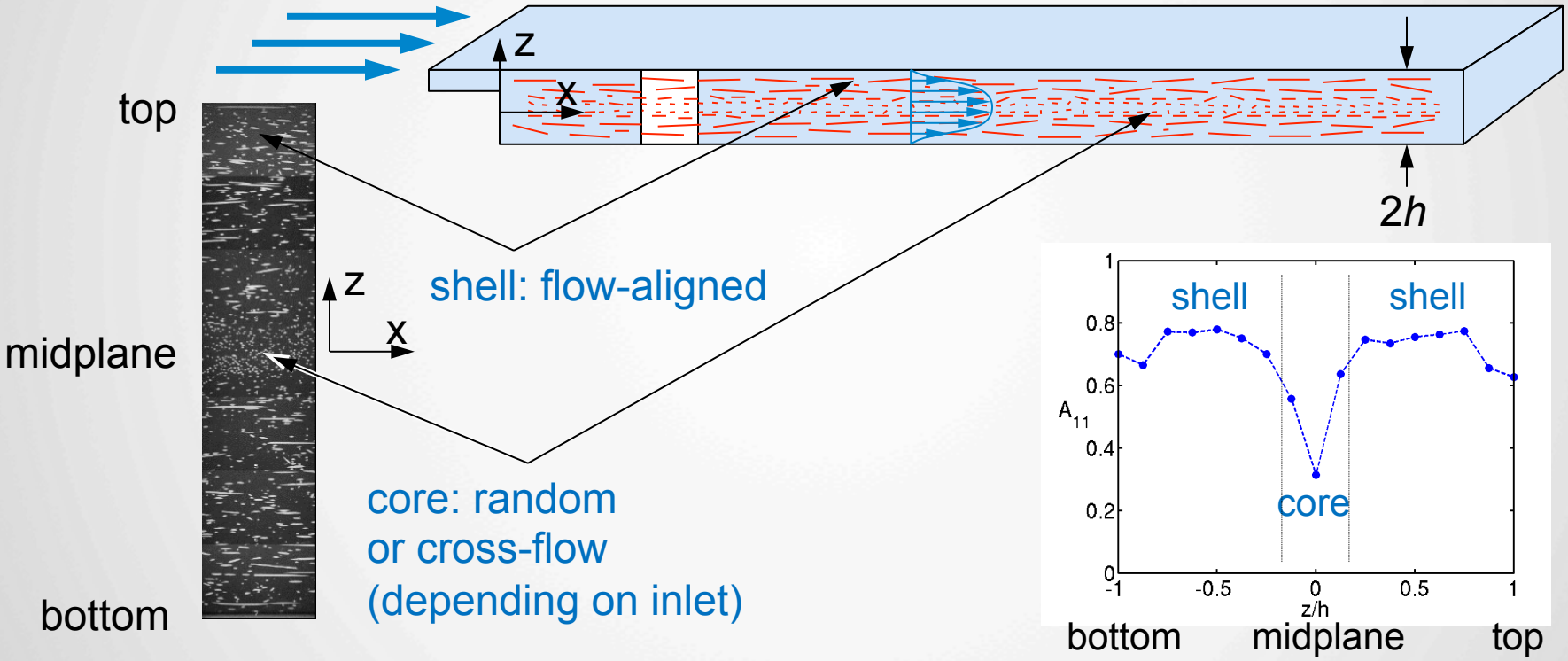

Example 2: If the flow is radial, the core is thicker and aligned in the cross-flow direction

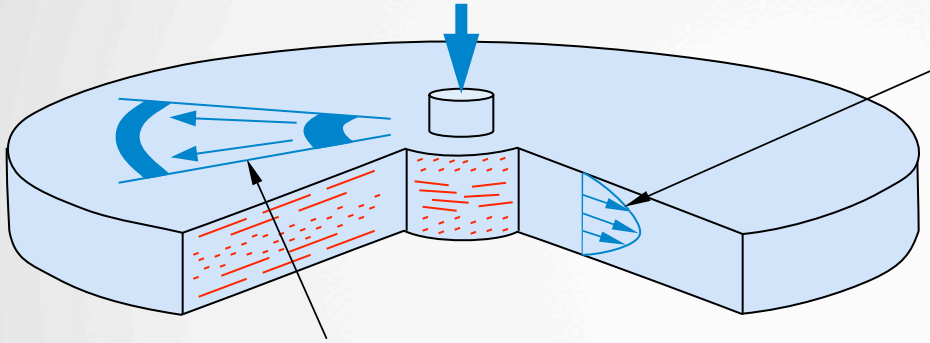

cross-gap shearing creates flow-aligned shell

in-plane stretching creates cross-flow core

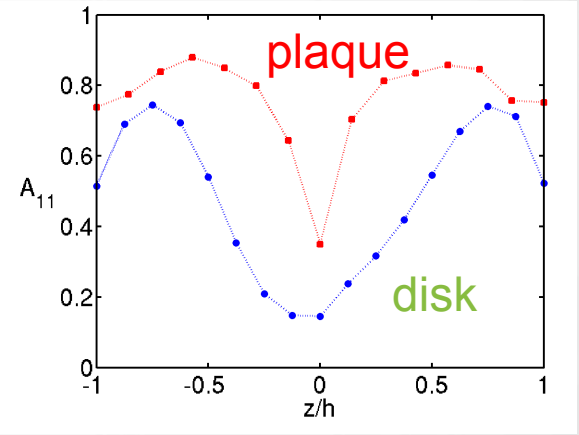

Example 3: Thicker plaques have thicker cores – this was a mystery!

2 mm thick

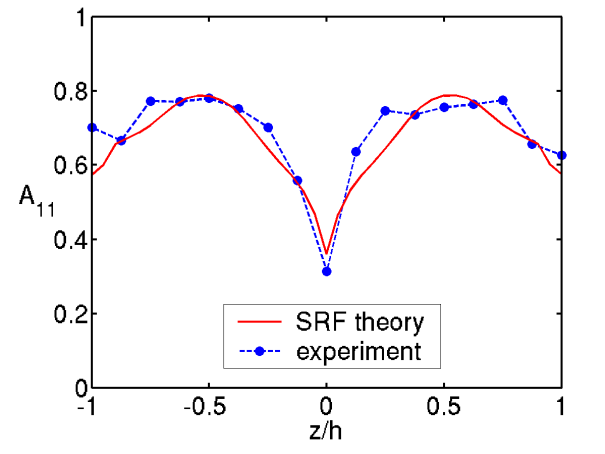

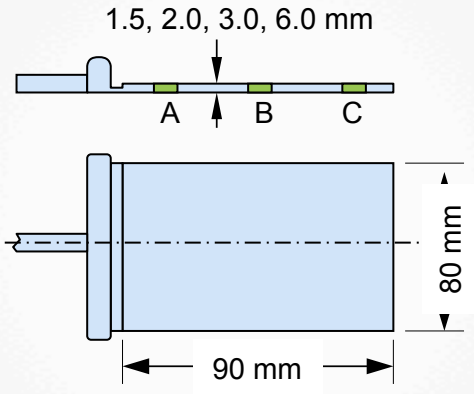

6 mm thick

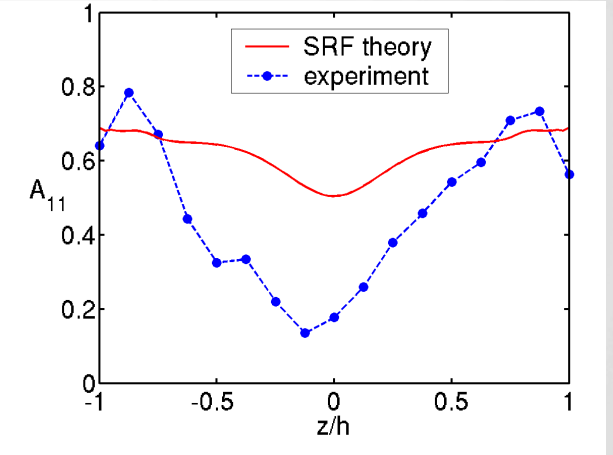

30 wt % glass fiber PBT (GE Valox 420)

Thin plaques fill as expected

- Short shots, 80×90×2 mm plaque

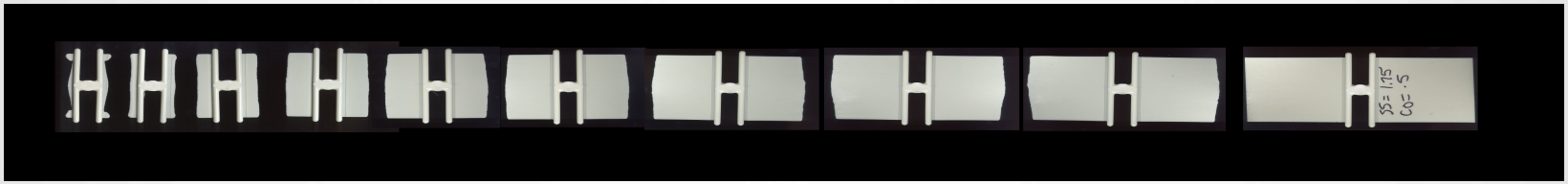

- Calculations assume top-view filling pattern like

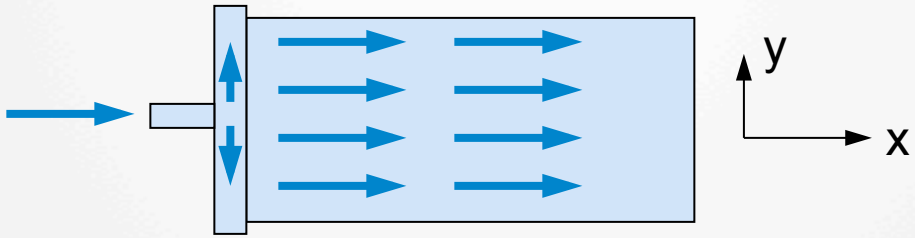

- Only thickness-direction (*xz*) shear is present: creates alignment in the flow direction (shell)

Thick plaques fill differently

- Short shots, 80×90×6 mm plaque

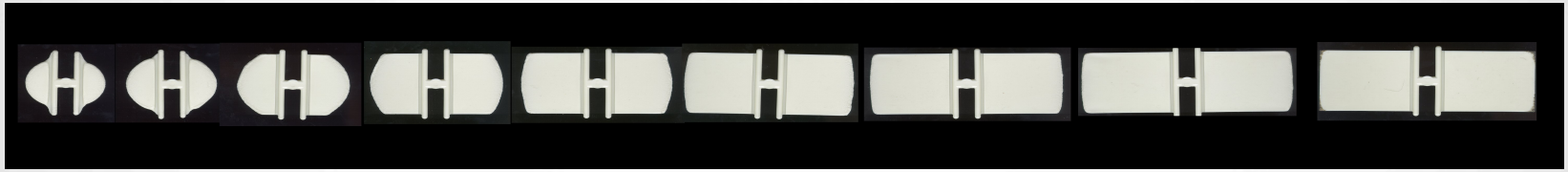

- Top-view filling pattern in thick plaque actually looks like

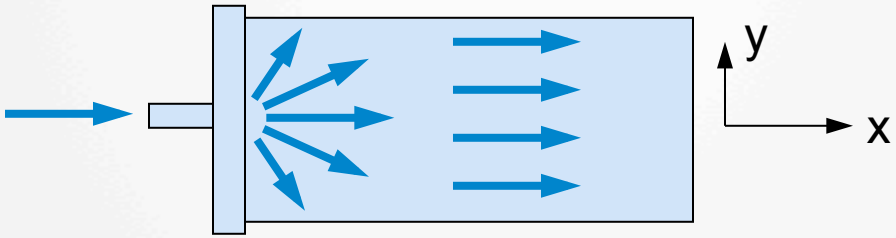

- **Radial flow near gate creates transversely aligned core**

Getting the flow pattern right allows the fiber orientation to be predicted correctly

Included radial flow near the gate

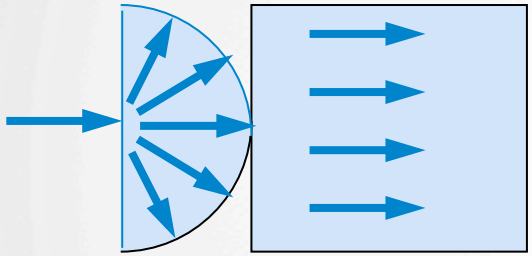

- 80×90×6 mm
- The mystery is solved!

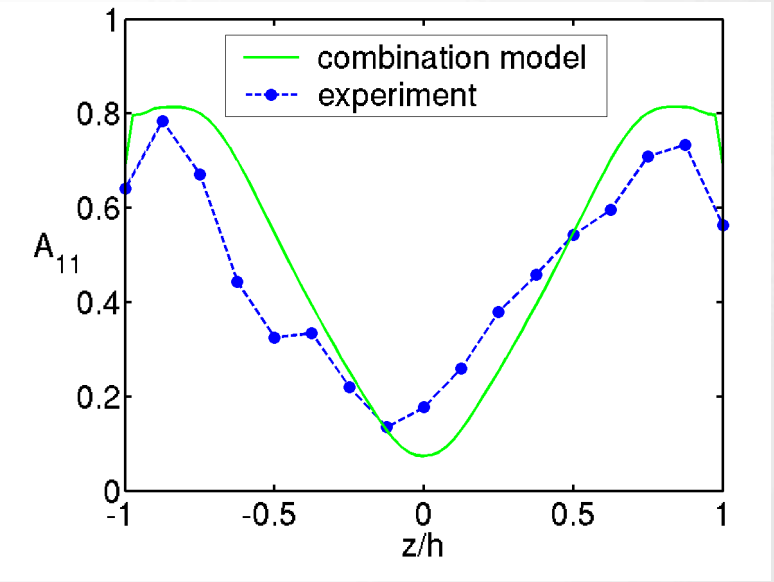

If Jeffery is always right qualitatively, then it's the quantitative aspects of orientation that matter

A vector p or angles (θ, ϕ) describe the orientation of a single fiber

- Rigid, axisymmetric fiber
- Unit vector **p** (or angles θ, ϕ)

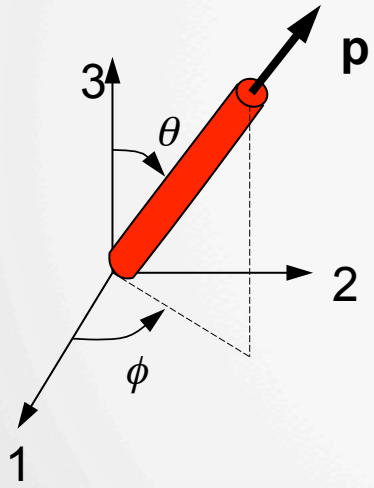

$$\mathbf{p} = \left\{ \begin{array}{c} p_1 \\ p_2 \\ p_3 \end{array} \right\} = \left\{ \begin{array}{c} \cos\phi \sin\theta \\ \sin\phi \sin\theta \\ \cos\theta \end{array} \right\}$$

$$p_1^2 + p_2^2 + p_3^2 = 1$$

Jeffery's equation quantitatively: fibers rotate in response to velocity gradients

$$\frac{d\mathbf{p}}{dt} = \mathbf{W}\cdot\mathbf{p} + \xi\left(\mathbf{D}\cdot\mathbf{p} - [\mathbf{p}\cdot\mathbf{D}\cdot\mathbf{p}]\,\mathbf{p}\right)$$

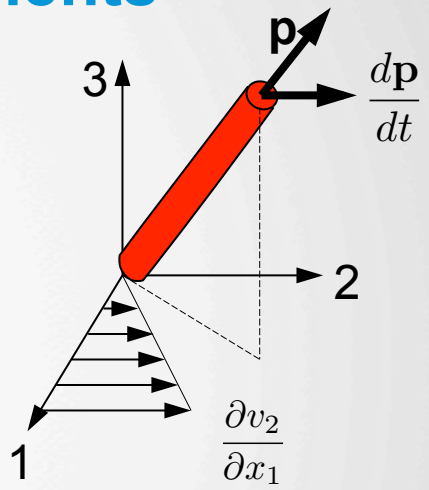

- Rate-of-deformation (fluid changing shape)

$$D_{ij} = \frac{1}{2}\left(\frac{\partial v_i}{\partial x_j} + \frac{\partial v_j}{\partial x_i}\right)$$

- Vorticity (rigid-body rotation)

$$W_{ij} = \frac{1}{2}\left(\frac{\partial v_i}{\partial x_j} - \frac{\partial v_j}{\partial x_i}\right)$$

ξ depends on the particle shape

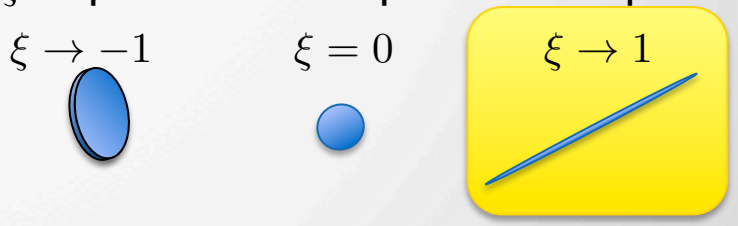

For single, rigid fibers, Jeffery's equation is perfect

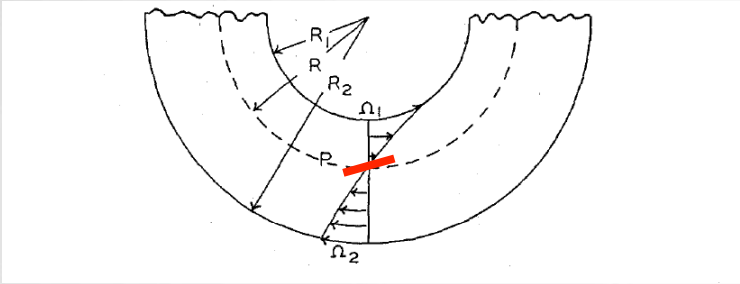

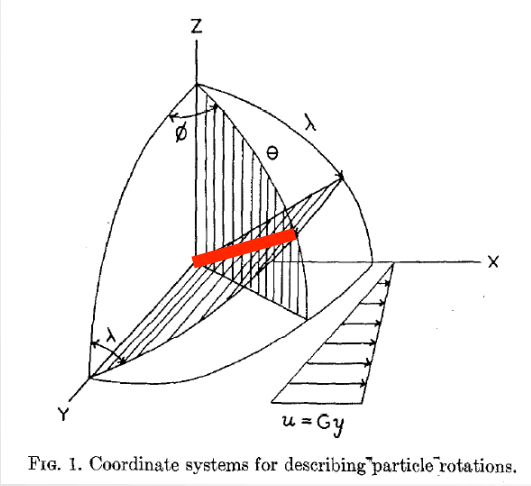

FIG. 1. Coordinate systems for describing particle rotations.

B. J. Trevelyan and S. G. Mason, *J. Colloid Sci., Vol. 6, pp 345-367, 1951.*

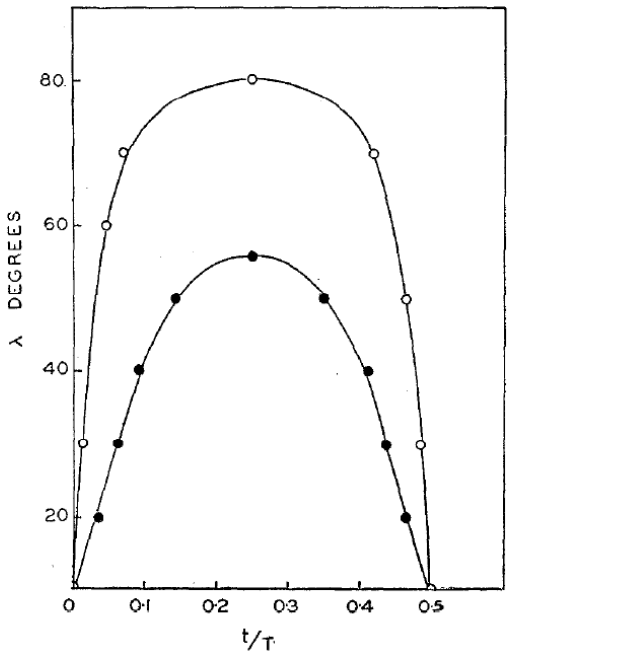

FIG. 7. Variation of angle λ with time of two different orbits (Table III) for a cylinder of axis ratio 66. The curves are calculated from Eq. [9].

An important property: Changing the shear rate changes only the rate of orientation, not the path

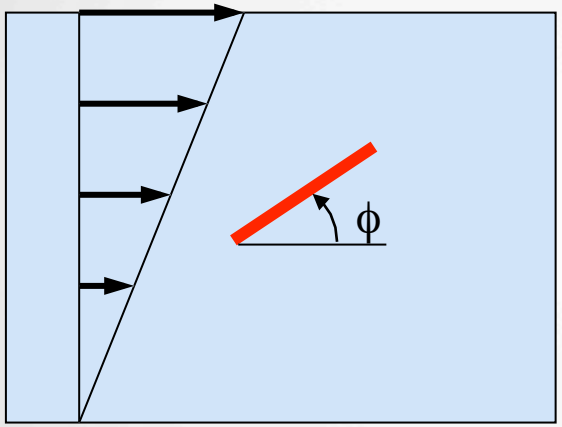

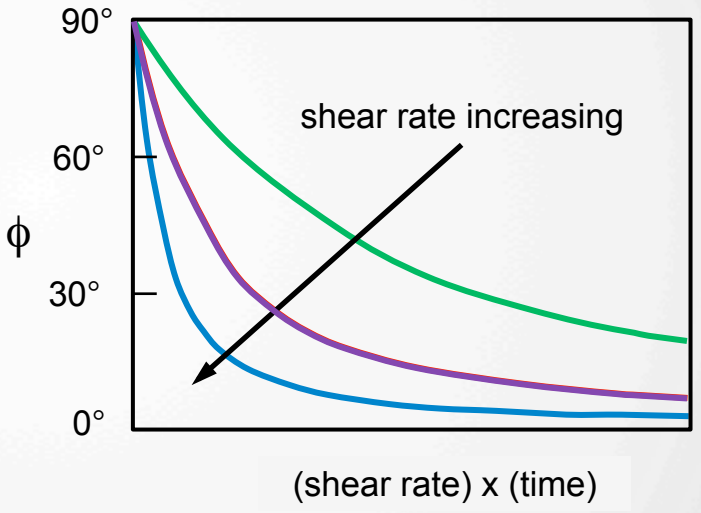

Problem 1: Fibers are never as well aligned as Jeffery says they should be, even after very large strains

Experiments by Folgar and Tucker (1983)

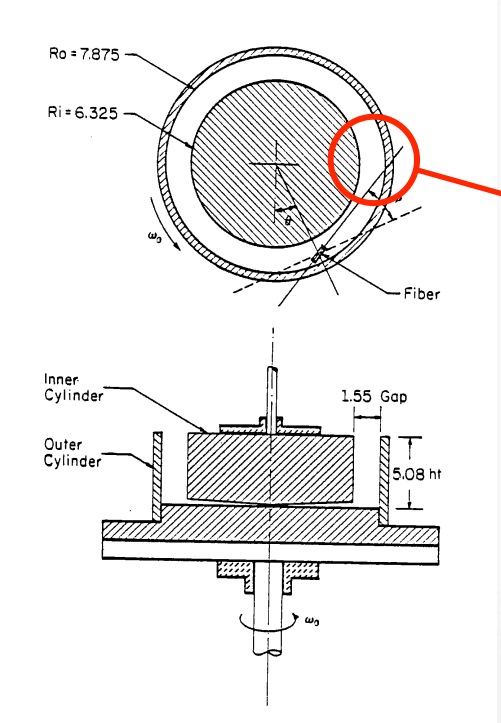

- Simple shear flow between concentric cylinders

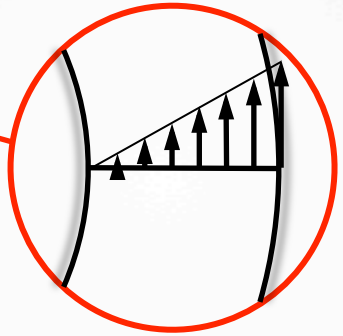

- Nylon fibers in silicone oil
- Pigmented tracer fibers

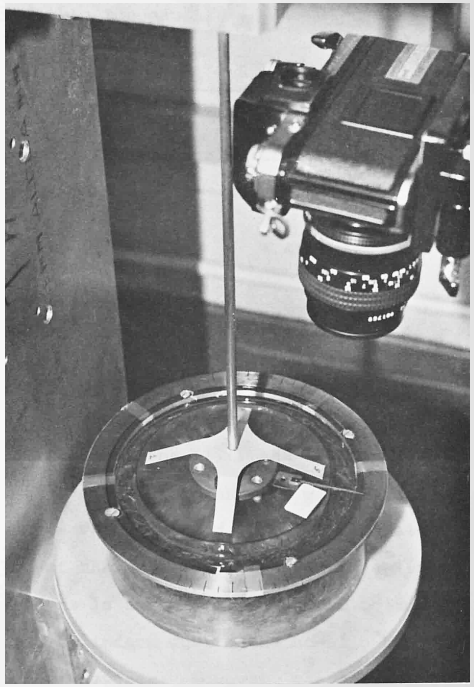

F. Folgar, PhD thesis, University of Illinois at Urbana-Champaign, 1983

The fibers never get fully aligned

F. Folgar, PhD thesis, University of Illinois at Urbana-Champaign, 1983

To model this, we add rotary diffusion to the model

- Fibers bump into one another
- Each fiber-fiber interaction moves the orientation of both fibers away from their Jeffery paths
- Many small, random changes add up to diffusive motion
- Make diffusivity proportional to shear rate

$\psi(\mathbf{p})$ is the fiber orientation distribution function

$$\psi \frac{d\mathbf{p}}{dt} = -\ (C_I \dot{\gamma})\ \frac{\partial \psi}{\partial \mathbf{p}} + \psi \left(\frac{d\mathbf{p}}{dt} \right)_{\text{Jeffery}}$$

Rotary diffusion moves fibers from regions of high orientation to regions of low orientation

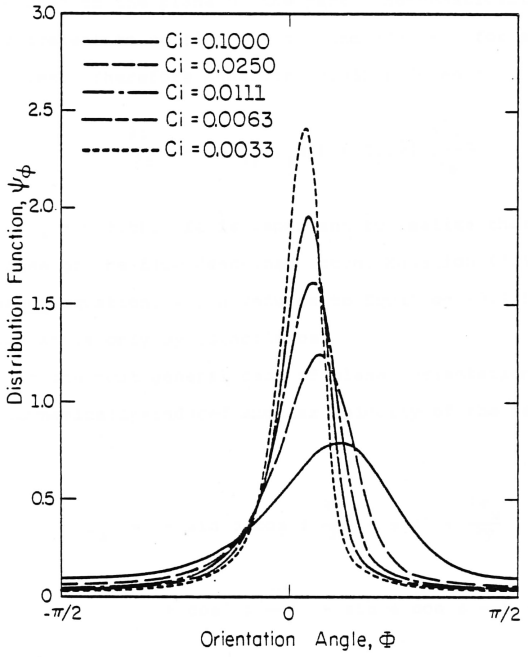

Larger C_I values give less-oriented steady state

F. Folgar, PhD thesis, University of Illinois at Urbana-Champaign, 1983

Adding a small amount of rotary diffusion gives a good fit to real orientation distributions

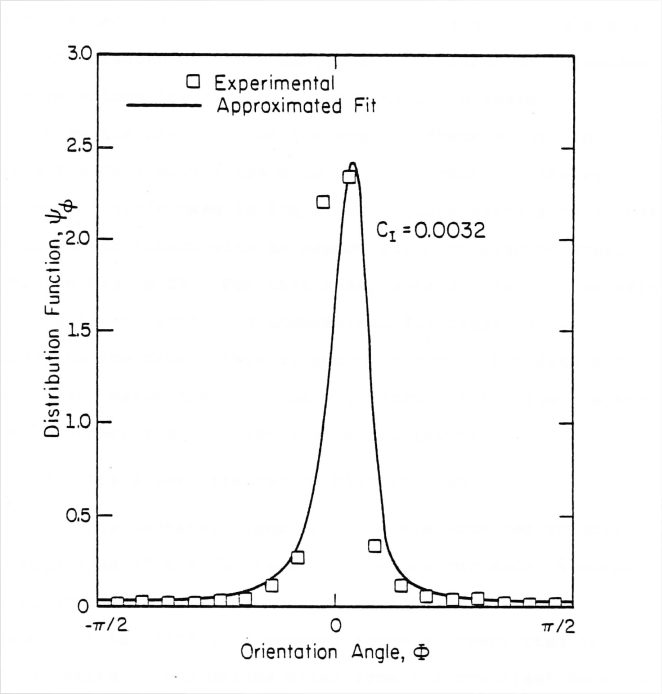

l/d = 83, volume fraction 0.04%

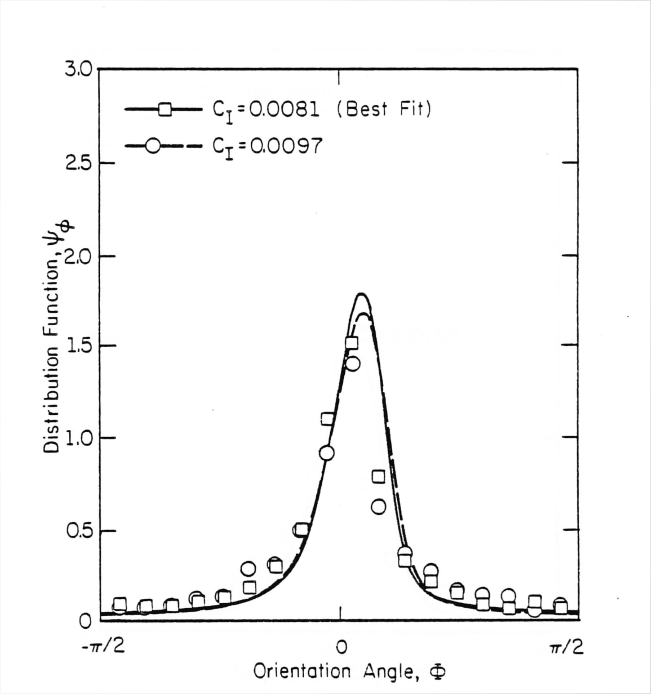

l/d = 16, volume fraction 8%
strains of 84 and 140

F. Folgar, PhD thesis, University of Illinois at Urbana-Champaign, 1983

Problem 2: Nobody can afford to compute a 3-D orientation distribution function in a real part

Solution: Use orientation tensors to describe the local orientation distribution

- Orientation tensor A_{ij}: ⟨average⟩ the products $p_i p_j$ for all fibers in the neighborhood

$$\mathbf{A} = \begin{bmatrix} A_{11} & A_{12} & A_{13} \\ A_{21} & A_{22} & A_{23} \\ A_{31} & A_{32} & A_{33} \end{bmatrix} = \begin{bmatrix} \langle p_1 p_1 \rangle & \langle p_1 p_2 \rangle & \langle p_1 p_3 \rangle \\ \langle p_2 p_1 \rangle & \langle p_2 p_2 \rangle & \langle p_2 p_3 \rangle \\ \langle p_3 p_1 \rangle & \langle p_3 p_2 \rangle & \langle p_3 p_3 \rangle \end{bmatrix}$$

example: $A_{33} = \langle cos^2\theta \rangle$

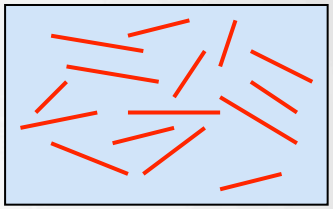

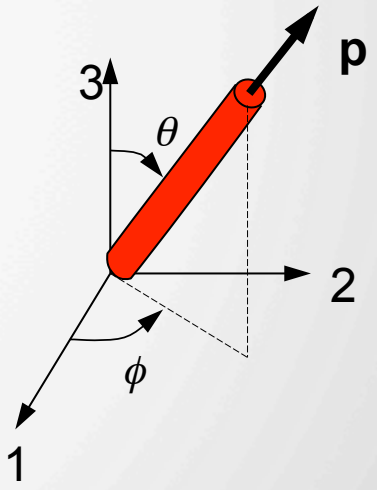

- 5 independent components, because $A_{ij} = A_{ji}$ and $A_{11} + A_{22} + A_{33} = 1$
- Also need fourth-order tensor, $\mathbb{A}_{ijkl} \equiv \langle p_i p_j p_j p_l \rangle$

Tensors capture the orientation state very efficiently

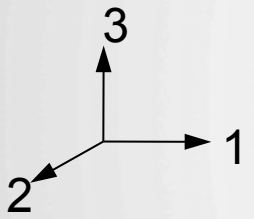

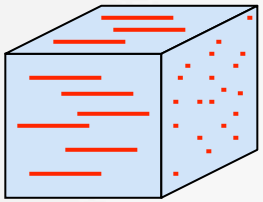

aligned

$$\mathbf{A} = \begin{bmatrix} 1 & 0 & 0 \\ 0 & 0 & 0 \\ 0 & 0 & 0 \end{bmatrix}$$

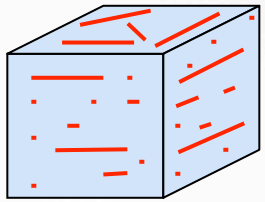

2-D random

$$\begin{bmatrix} 0.5 & 0 & 0 \\ 0 & 0.5 & 0 \\ 0 & 0 & 0 \end{bmatrix}$$

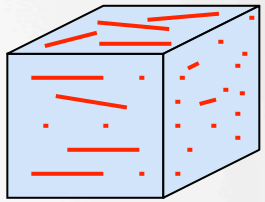

shell layer

$$\begin{bmatrix} 0.81 & 0.00 & -0.01 \\ 0.00 & 0.16 & 0.00 \\ -0.01 & 0.00 & 0.03 \end{bmatrix}$$

Tensors also give principal directions of orientation

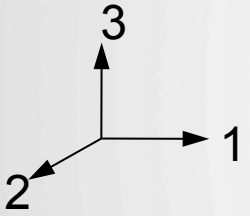

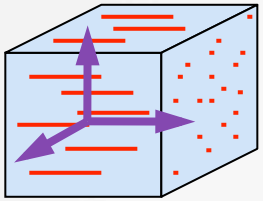

aligned

$$\mathbf{A} = \begin{bmatrix} 1 & 0 & 0 \\ 0 & 0 & 0 \\ 0 & 0 & 0 \end{bmatrix}$$

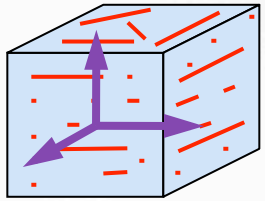

2-D random

$$\begin{bmatrix} 0.5 & 0 & 0 \\ 0 & 0.5 & 0 \\ 0 & 0 & 0 \end{bmatrix}$$

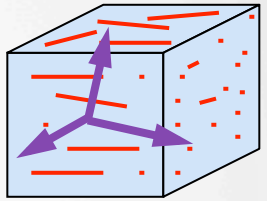

shell layer

$$\begin{bmatrix} 0.81 & 0.00 & -0.01 \\ 0.00 & 0.16 & 0.00 \\ -0.01 & 0.00 & 0.03 \end{bmatrix}$$

We can re-write the Jeffery/Folgar-Tucker equation in terms of orientation tensors

- Equivalent evolution equation for orientation tensor (Advani & Tucker 1987):

$$\dot{\mathbf{A}} = (\mathbf{W}\cdot\mathbf{A} - \mathbf{A}\cdot\mathbf{W}) + \xi\,(\mathbf{D}\cdot\mathbf{A} + \mathbf{A}\cdot\mathbf{D} - 2\mathbb{A}:\mathbf{D}) + 2C_I\dot{\gamma}\,(\mathbf{I} - 3\mathbf{A})$$

- Use a closure approximation for the fourth-order tensor $\mathbb{A} = f(\mathbf{A})$

- Larger values of C_I values give less alignment at steady state

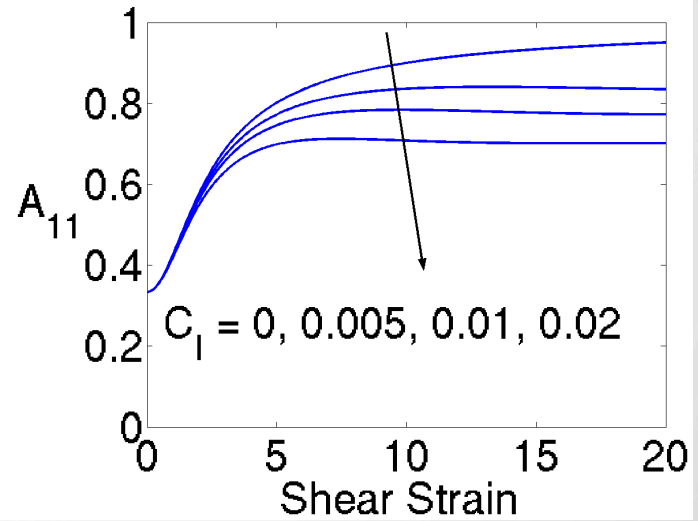

Putting this to work:

- Ignore the core orientation (and ignore surface skins, if you have them)
- Adjust C_I to match flow-direction alignment (A_{11}) in the shell layer (steady state orientation in simple shear flow)

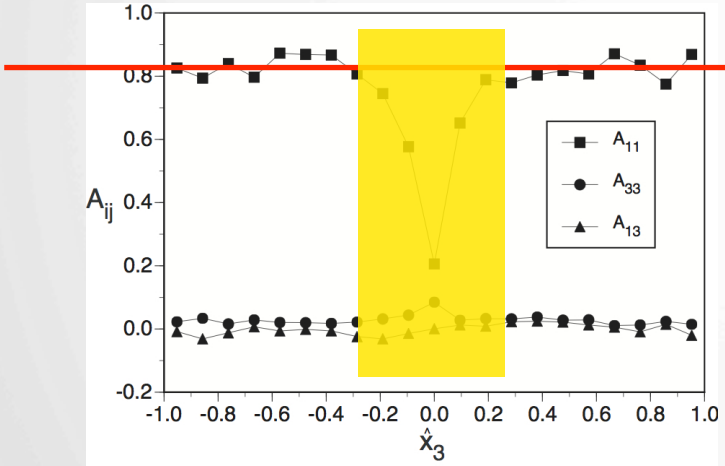

Polycarbonate, 30% glass (Lexan LS2)

$A_{11} = 0.83 \rightarrow C_I = 0.020$

$$\mathbf{A} = \begin{bmatrix} 0.830 & 0.000 & -0.134 \\ 0.000 & 0.097 & 0.000 \\ -0.134 & 0.000 & 0.073 \end{bmatrix}$$

- No choice on other components of **A**
- Value of C_I depends on closure approximation (here: hybrid)

Problem 3: Fibers align much slower than Jeffery predicts ("slow orientation kinetics")

Symptom: Property predictions good for long flow lengths, but poor for short flows

- Edge-gated strips, PBT 30% glass fiber
- Measure elastic modulus in flow (E_{11}) and crossflow (E_{22}) directions
- Predict modulus using **predicted** fiber orientation

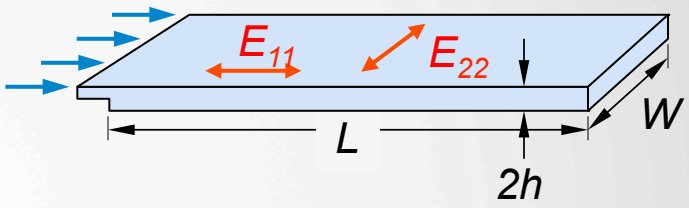

$W \times L \times 2h$ (mm)		Experimental (GPa)	Predicted (GPa)
76×279×3	E_{11}	8.8	8.6
76×279×3	E_{22}	4.6	4.3
75×**125**×3	E_{11}	7.7	**8.6**
75×**125**×3	E_{22}	5.4	**4.3**

Problem: the standard model under-predicts core thickness in a short plaque

- Leads to over-prediction of E_{11}, under-prediction of E_{22}

  - 30 wt % glass fiber PBT (GE Valox-420-1001)
  - 80×90×2 mm
  - slow fill speed

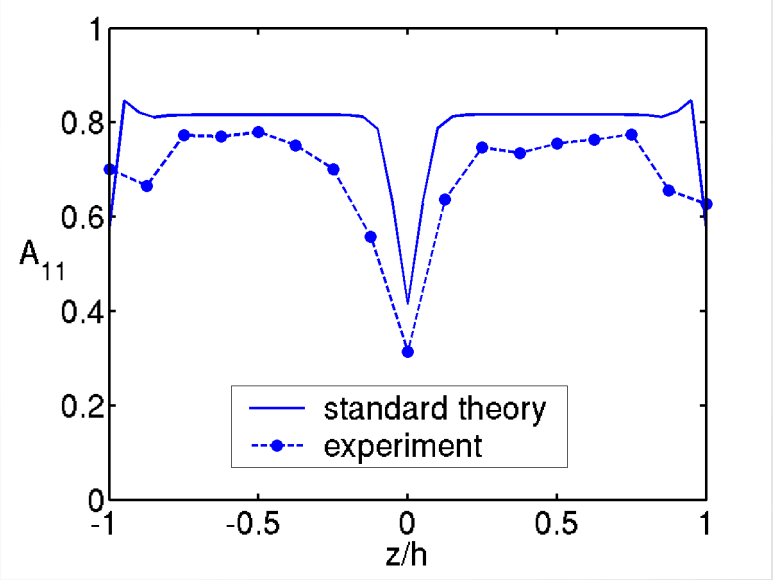

Thicker cores in plaques imply slow orientation kinetics in simple shear

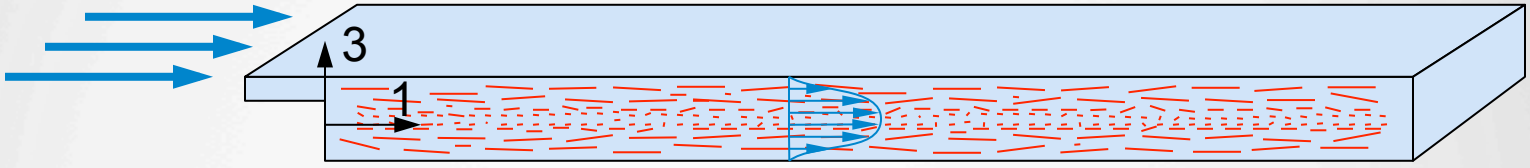

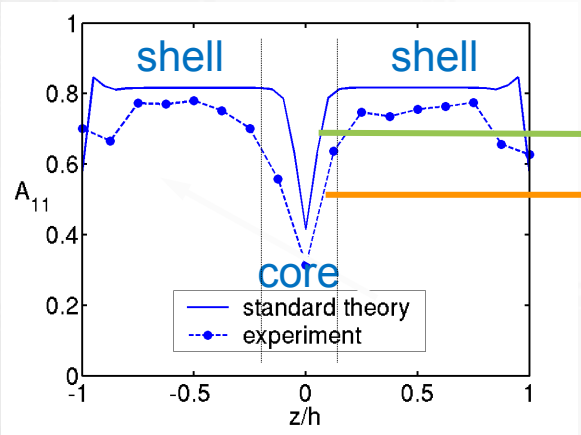

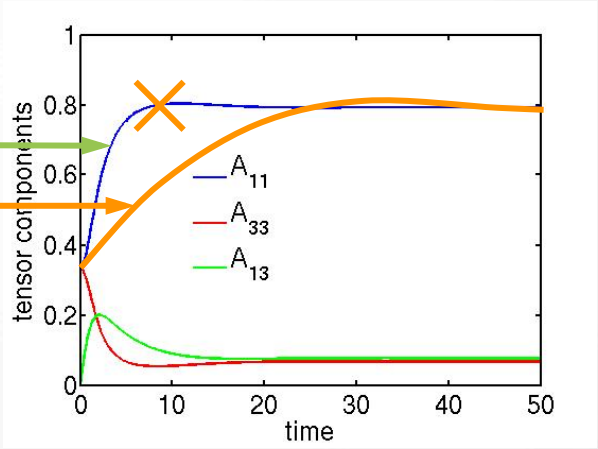

bottom midplane top

simple shear flow, C_I = 0.008

SRF theory allows fiber orientation to develop more slowly

- Hypothesis: fibers experience local strain that is lower than average
  - resin-rich “slip layers” absorb most of the strain
  - fibers follow Jeffery-type motion based on local strain rate
- Strain Reduction Factor (SRF) = (fiber strain rate / total strain rate)

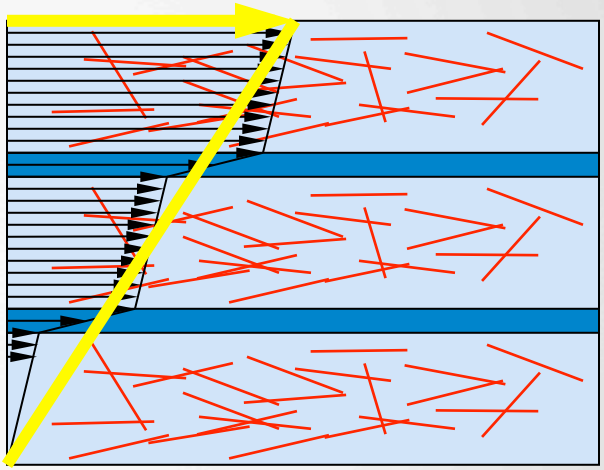

$$\dot{\mathbf{A}} = \frac{1}{\mathrm{SRF}}\left[\mathbf{W}\cdot\mathbf{A} - \mathbf{A}\cdot\mathbf{W} + \xi(\mathbf{D}\cdot\mathbf{A} + \mathbf{A}\cdot\mathbf{D} - 2\mathbf{D}:\mathbb{A}) + 2C_I\dot{\gamma}(\mathbf{I} - 3\mathbf{A})\right]$$

SRF theory does a good job for short plaques . . .

- Fit data by choosing SRF=20
  - PBT, 30% glass
  - 80×90×2 mm
  - slow fill speed

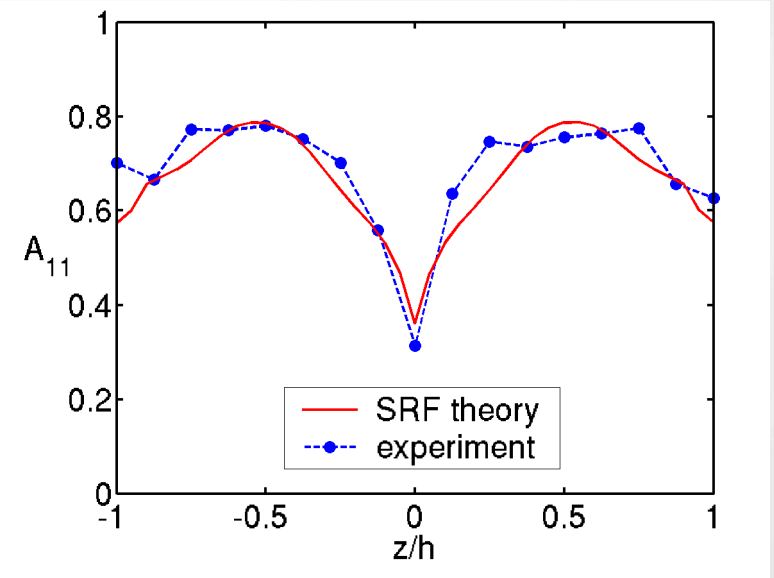

. . . but SRF also does some crazy things

- Example: SRF does not behave sensibly in rigid-body rotation

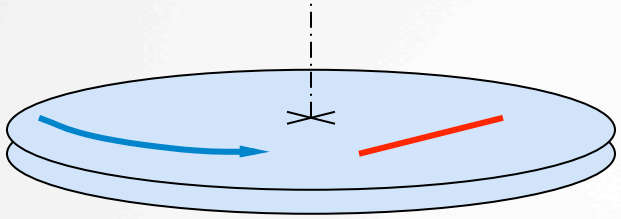

flow rotates at 100 RPM

$$\dot{\mathbf{A}} = \frac{1}{\mathrm{SRF}}\left[\mathbf{W}\cdot\mathbf{A} - \mathbf{A}\cdot\mathbf{W}\right]$$

if SRF = 20, fiber rotates at 5 RPM!

- SRF theory is not reliable in general 3D flows
- Need an **objective** model that gives similar predictions

To build a better theory, use the idea of principal directions and principal values for orientation

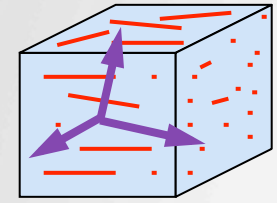

keep the same

rotation of principal directions

change in **A**

slow down by κ = (1/SRF)

change in principal values

new eqn for **A**

RSC model
(Reduced Strain Closure)

- Behaves like SRF in simple shear
- Doesn't have any crazy behaviors

RSC gives good predictions for short-fiber moldings

PBT, 30% glass, κ = 1/20

3mm thick ISO plaque, slow fill

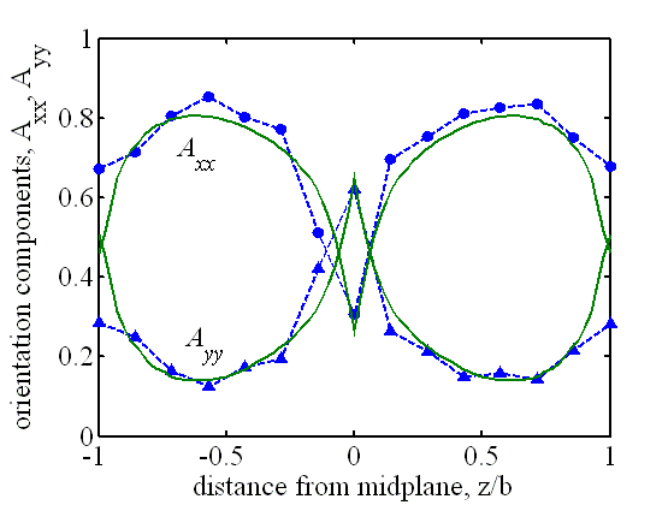

1.5mm thick disk, fast filling

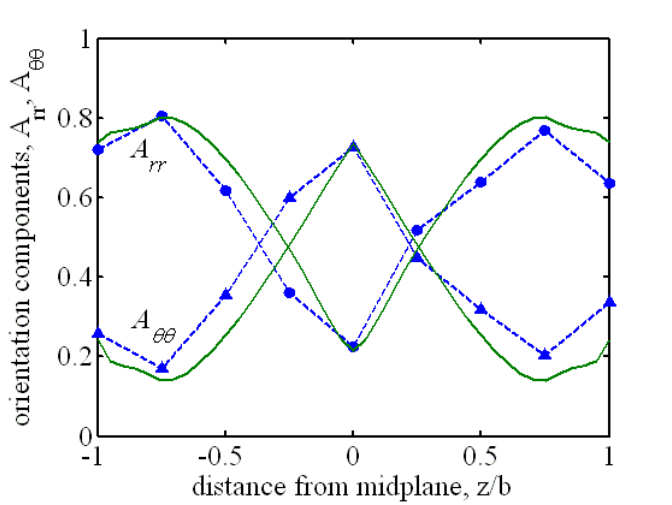

Putting this to work (RSC)

- Use C_l to set A_{11} in the shell layer (same as before)
- Increase SRF until core width is reasonable (κ = 1/10 to 1/30 is common)
- Downstream results will be more sensitive to orientation just inside the gate

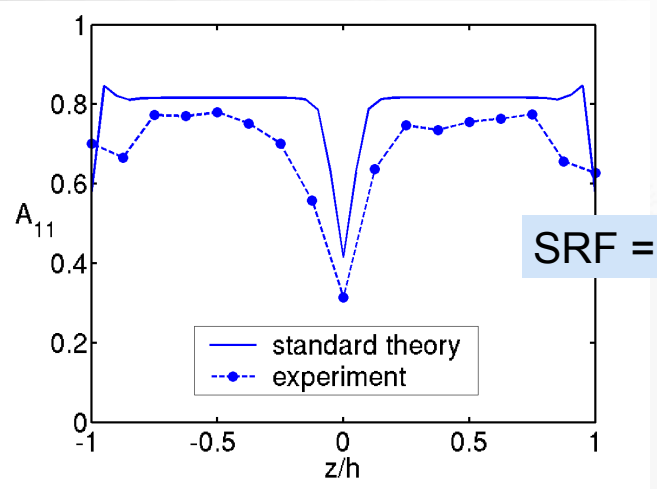

SRF = 1

SRF = 20

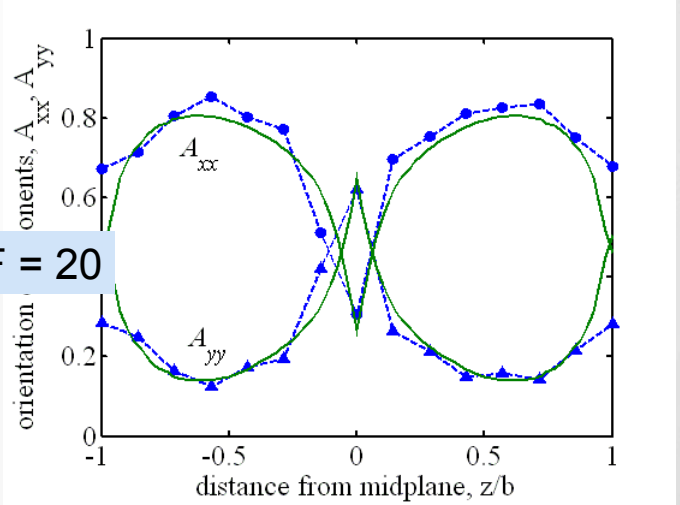

Problem 4: Long-fiber materials behave differently

Long-fiber thermoplastics (LFTs) have lower shell alignment, thicker cores than short-fiber materials

SFT

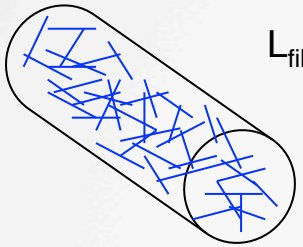

L_{fiber} = 0.2-0.4 mm

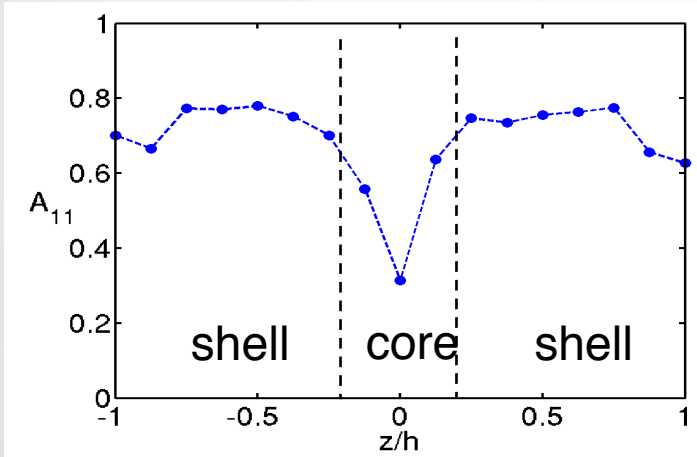

LFT

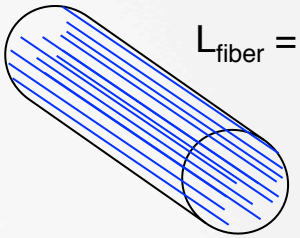

L_{fiber} = 10-13 mm

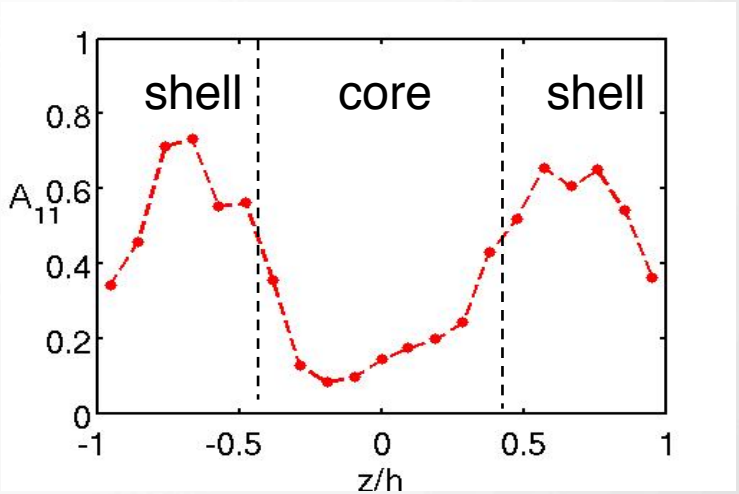

RSC can predict some components, but not all

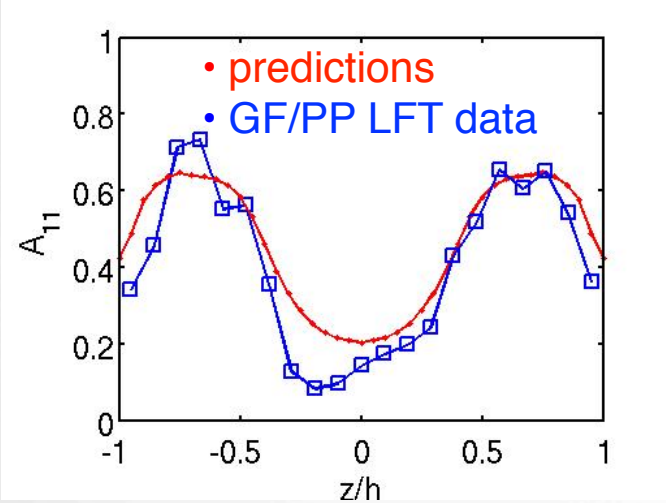

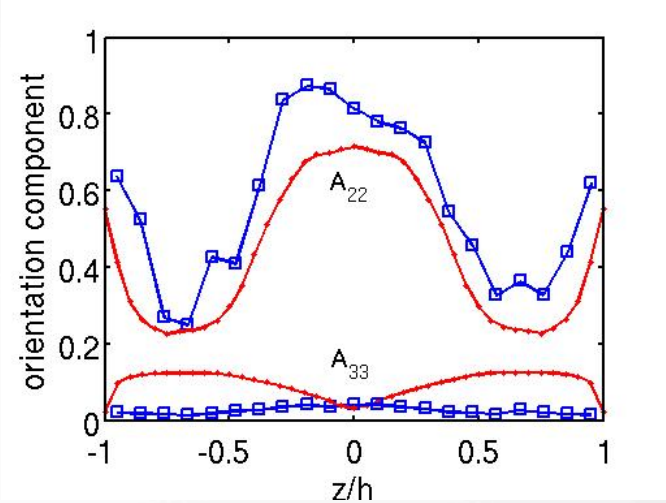

- Slow-filled, glass-polypropylene, 3 mm thick, ISO plaque
- RSC model, κ = 1/30, C_I = 0.03

Idea for improving the model: anisotropic rotary diffusion (ARD)

- Folgar-Tucker and RSC models assume that fiber-fiber interactions cause **isotropic rotary diffusion** -- arbitrary!

$$\dot{\mathbf{A}} = (\mathbf{W}\cdot\mathbf{A} - \mathbf{A}\cdot\mathbf{W}) + \xi(\mathbf{D}\cdot\mathbf{A} + \mathbf{A}\cdot\mathbf{D} - 2\mathbb{A}:\mathbf{D}) + 2C_I\dot{\gamma}(\mathbf{I} - 3\mathbf{A})$$

  - C_I is a scalar

- **Anisotropic rotary diffusion** is more general
  - replace scalar C_I with tensor $\mathbf{C}$
  - how to write the math?

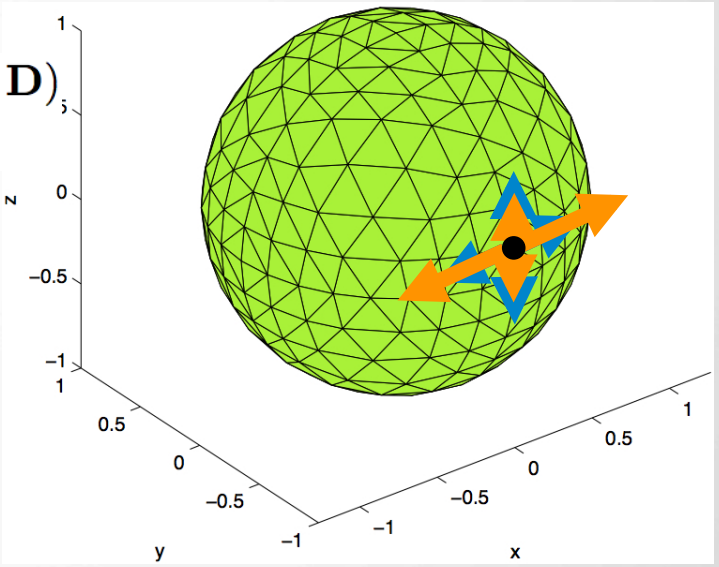

The ARD model has five parameters in place of C_I (!)

$$\dot{\mathbf{A}} = (\mathbf{W}\cdot\mathbf{A} - \mathbf{A}\cdot\mathbf{W}) + \xi(\mathbf{D}\cdot\mathbf{A} + \mathbf{A}\cdot\mathbf{D} - 2\mathbb{A}:\mathbf{D}) + \dot{\gamma}(2\mathbf{C} - 2(\mathrm{tr}\mathbf{C})\mathbf{A} - 5(\mathbf{C}\cdot\mathbf{A} + \mathbf{A}\cdot\mathbf{C}) + 10\mathbb{A}:\mathbf{C})$$

- Interaction coefficient C_I is replaced by **C** tensor
- **C** can depend on orientation state and flow type (e.g., shear vs. elongation)

$$\mathbf{C} = b_1\mathbf{I} + b_2\mathbf{A} + b_3\mathbf{A}^2 + b_4\frac{\mathbf{D}}{\dot{\gamma}} + b_5\frac{\mathbf{D}^2}{\dot{\gamma}^2}$$

- Actually use ARD with RSC

ARD/RSC model gives good agreement with LFT experimental data

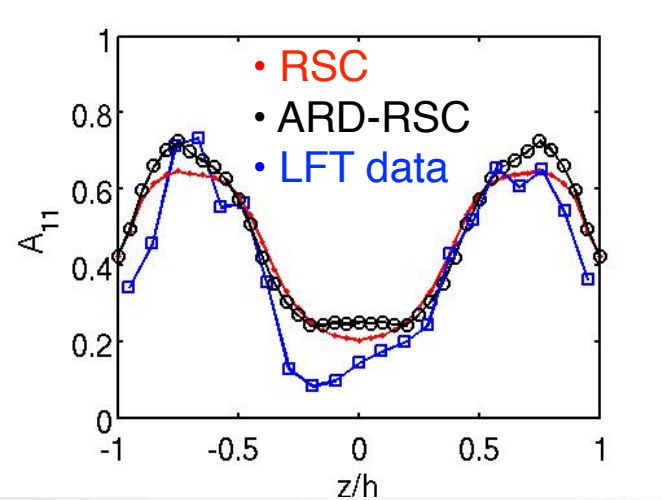

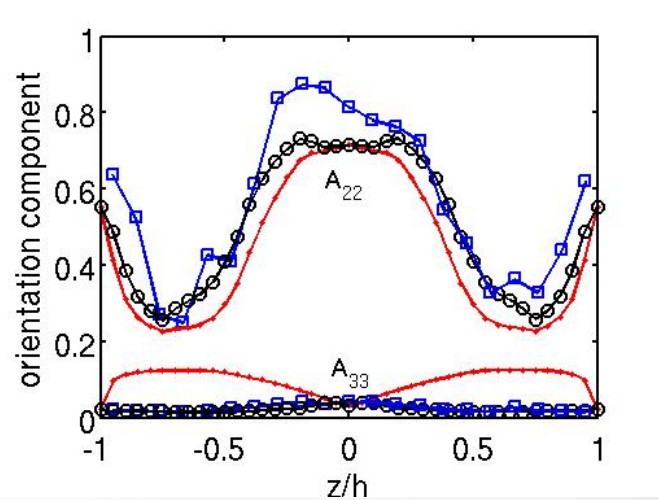

- κ = 1/30, b_i = (0.0007848, 0.02357, 0.01, 0.000011676, -0.003)
- Slow-filled, glass-polypropylene, 3 mm thick, ISO plaque

But poor choices of ARD parameters can give non-physical behaviors

- Startup of simple shear flow

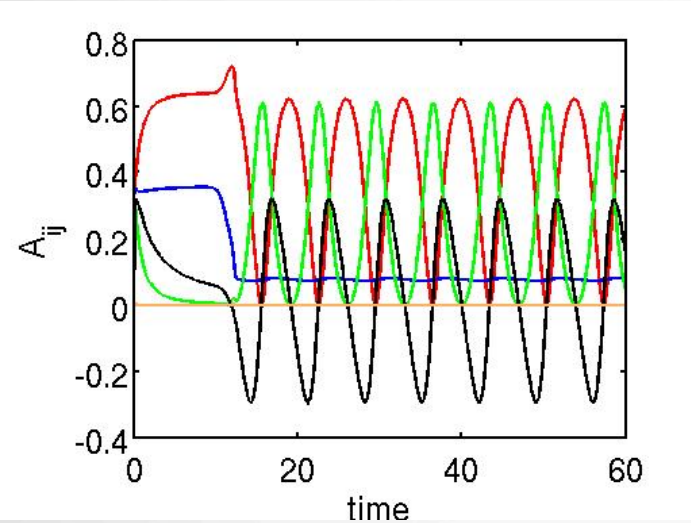

- A_{11}
- A_{22}
- A_{33}
- A_{31}
- A_{23}, A_{12}

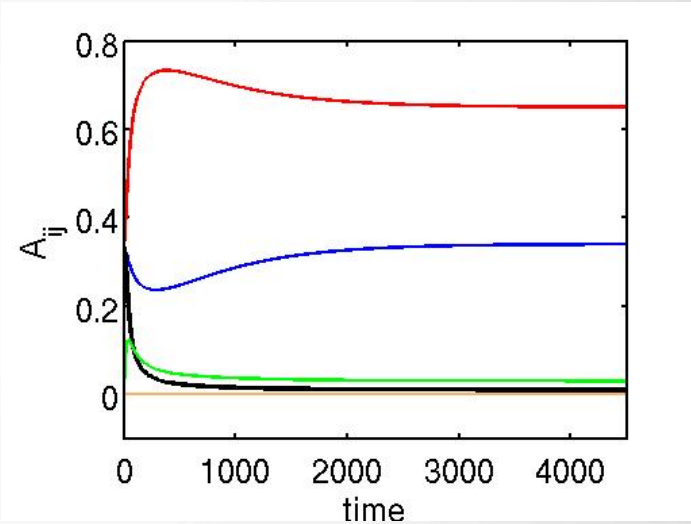

Putting this to work (ARD):

- Need values for five parameters: *b1, b_2, b_3, b_4, b_5*
- Select a target orientation **tensor** in the shell layer (steady state in simple shear flow). This fixes three parameters

$$\mathbf{A}^{\exp} = \begin{bmatrix} 0.65 & 0 & 0.03 \\ 0 & 0.34 & 0 \\ 0.03 & 0 & 0.01 \end{bmatrix}$$

flow direction
thickness direction
tilt

- Remaining two parameters are chosen to guarantee good behavior:
  - orientation is stable in steady simple shear flow
  - diffusivity is always positive
  - solutions are physically valid for other flows (planar & biaxial elongation)
- Only use ARD parameters that have been tested – **no guessing!**

Class summary: modeling fiber orientation

- Two rules from Jeffery explain everything qualitatively:
  - shearing flows align fibers in the direction of flow
  - stretching flows align fiber in the direction of stretching
- Orientation tensors make the computation affordable
- For short-fiber materials:
  - set CI to get correct flow-direction alignment in shell
  - set RSC factor to get correct core thickness
- For long-fiber materials:
  - can use ARD to s etthree orientation components in shell
  - set RSC factor to get correct core thickness

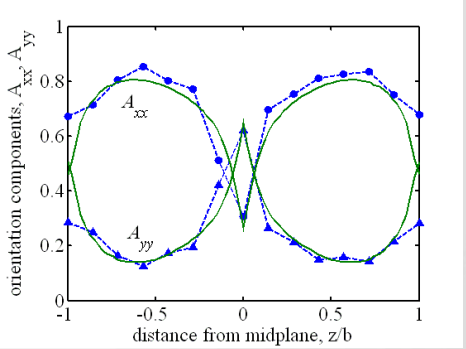

There can be significant fiber attrition during LFT processing

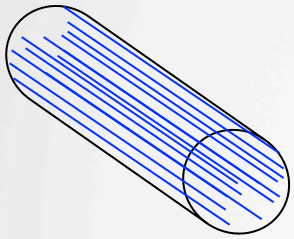

pellet

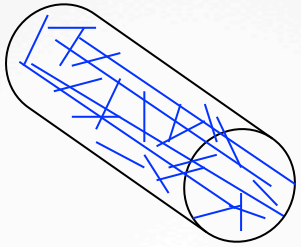

careful processing

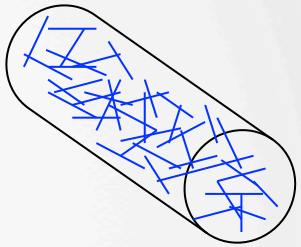

poor processing

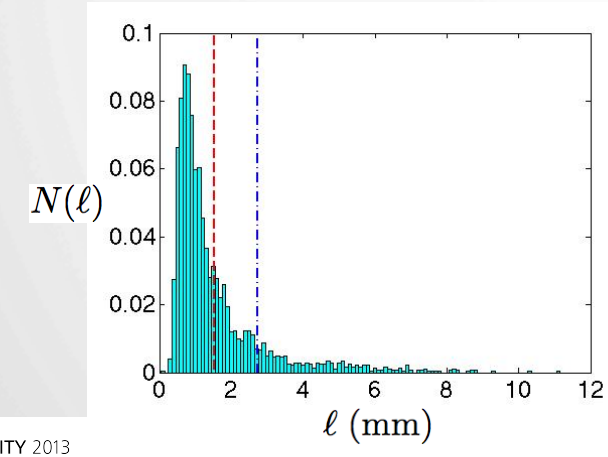

- Fiber breakage increases with increasing stress and total strain
- No quantitative model for fiber length distributions has existed before

Our fiber breakage model starts from the very beginning

Phenomena

- More stress, more strain = more breakage
- Broad distribution of fiber length
- Long fibers more likely to break

Strategy

- Choose variables to quantify the microstructure
- Identify conservation laws that these variables must obey
- Develop constitutive models for the remaining dynamical aspects of microstructure development

A fiber length distribution (FLD) quantifies the microstructure

- Use discrete lengths: $\ell_i = i\,\Delta\ell$
- N_i = number of fibers per unit volume with length ℓ_i
- $N_i, i = 1 \text{ to } i_{max}$, describes the full FLD
- Number-average and weight-average lengths provide a convenient summary

$$\bar{L}_n = \frac{\sum N_i \ell_i}{\sum N_i} \qquad \bar{L}_w = \frac{\sum N_i \ell_i^2}{\sum N_i \ell_i}$$

$$\bar{L}_w \geq \bar{L}_n$$

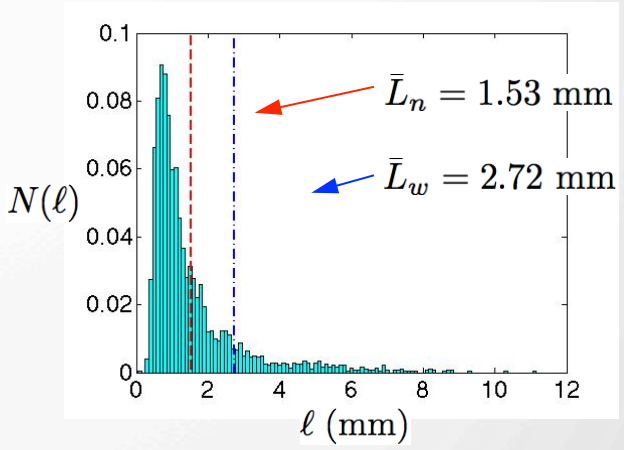

Define breakage rates for both parent and child fibers

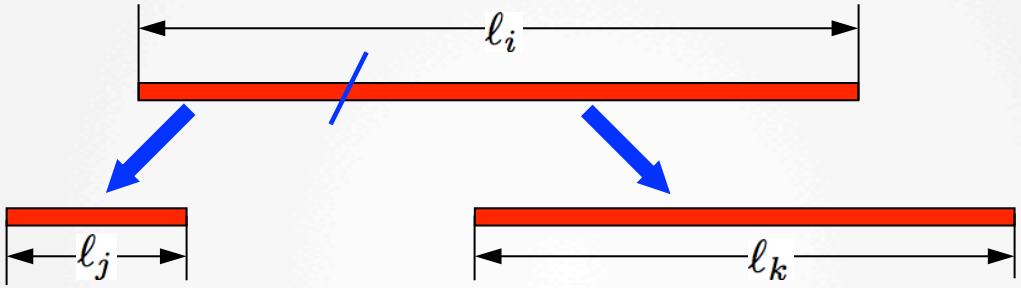

- $P_i\,\Delta t$ = probability of breaking a parent w/ length ℓ_i in time Δt
- $R_{ji}\,\Delta t$ = probability of creating a child w/ ℓ_j from a parent w/ ℓ_i
- Mass conservation and symmetry require:

$$\sum_j R_{ji} = 2P_i$$

$$R_{ki} = R_{(i-k)i}$$

$$\text{e.g., } R_{6,10} = R_{4,10}$$

The fiber length distribution must obey a mass conservation equation

$$\underbrace{\frac{dN_i}{dt}}_{\text{change in}} = \underbrace{-P_i N_i}_{\text{loss by breaking}} + \underbrace{\sum_k R_{ik} N_k}_{\text{gain by creating}}$$

change in fibers of length l_i

loss by breaking parents w/ l_i

gain by creating children w/ l_i

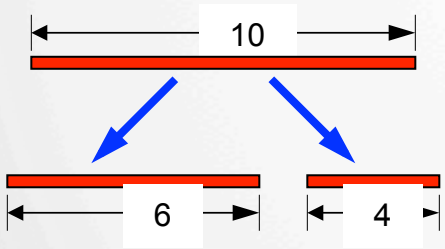

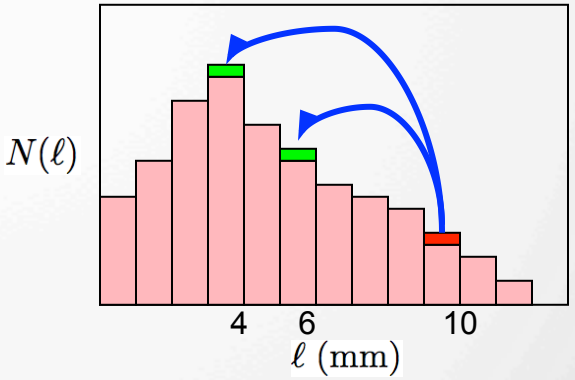

Typical hydrodynamic forces can break fibers only by buckling[1]

- In simple shear, fibers are periodically loaded in compression

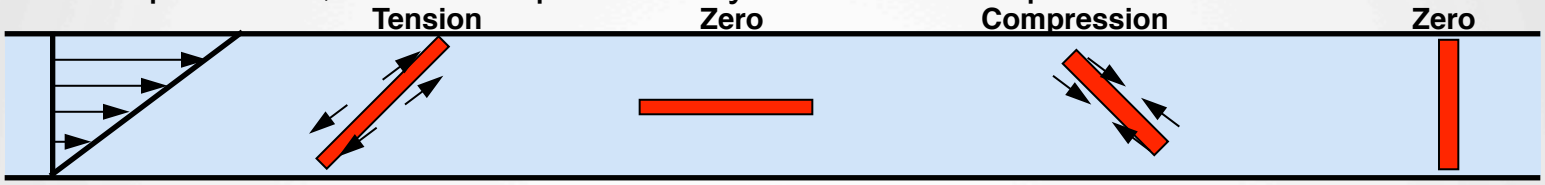

- Dinh and Armstrong (1984) gives hydrodynamic compressive force F_i at center of fiber of length l_i (ζ is a drag coefficient)

$$F_i = \frac{\zeta \eta_m \ell_i^2}{8}(-\mathbf{D} : \mathbf{pp})$$

- Classical Euler buckling theory gives critical buckling force

$$F_{\text{crit}} = \frac{\pi^3 E_f d_f^4}{64 l_i^2}$$

[1]Forgacs and Mason, 1959; Salinas and Pittman, 1981; von Turkovich and Erwin, 1983

Hydrodynamic buckling depends on stress and orientation

- For a fiber of length ℓ_i, expect buckling if

$$\frac{F_i(\mathbf{p})}{F_{\text{crit}}} = \hat{\dot{\gamma}}_i(-2\hat{\mathbf{D}} : \mathbf{pp}) \geq 1$$

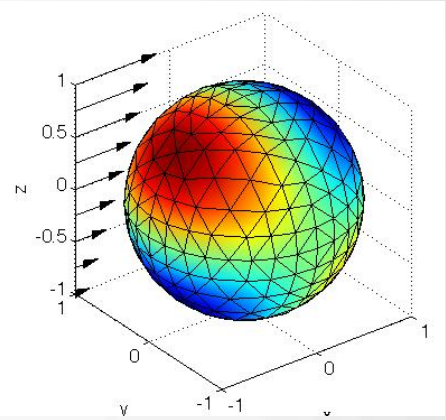

- Dimensionless shear rate and $\mathbf{D}$ tensor

$$\hat{\dot{\gamma}}_i \equiv \frac{4\zeta\eta_m\dot{\gamma}\ell_i^4}{\pi^3 E_f d_f^4} \qquad \hat{\mathbf{D}} \equiv \mathbf{D}/\dot{\gamma}$$

  - longer fibers break more easily
  - higher stresses produce more breakage
  - stiffer fibers resist buckling (carbon vs. glass)

Combine buckling formula and orientation distribution to give breakage rate

- Postulate breakage rate (breakage probability) of

$$P_i = C_B\dot{\gamma} \times (\text{fraction of fibers with } F_i(\mathbf{p})/F_{crit} \geq 1)$$

- Evaluate numerically using orientation in steady simple shear
- A good approximation to the result is

$$P_i = C_B\dot{\gamma}\left[1 - \exp(1 - \hat{\dot{\gamma}}_i)\right]$$

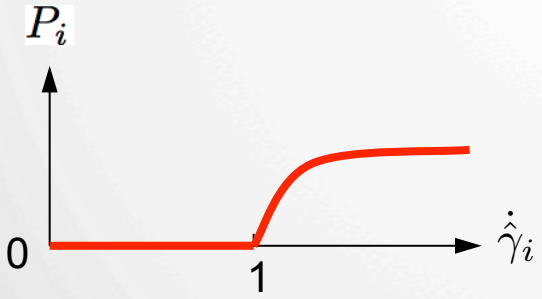

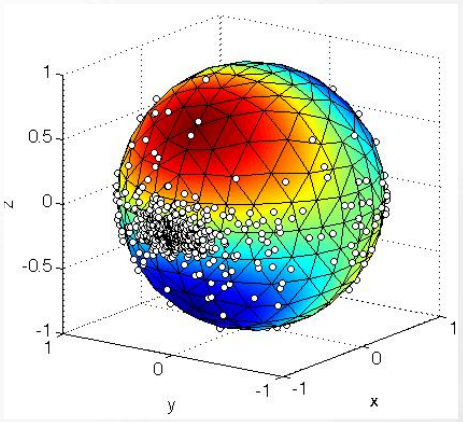

Where along the fiber does the break occur? Guess a Gaussian distribution

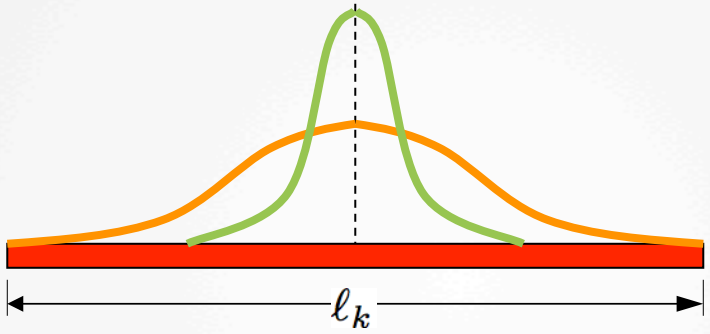

- R_{ik} is Gaussian with mean $\ell_k/2$ and standard deviation $S\ell_k$
- Normalized by $\int R_{ik}\, d\ell_i = 2P_k$
- S parameter controls distribution of child fiber lengths

The model gives reasonable-looking FLDs

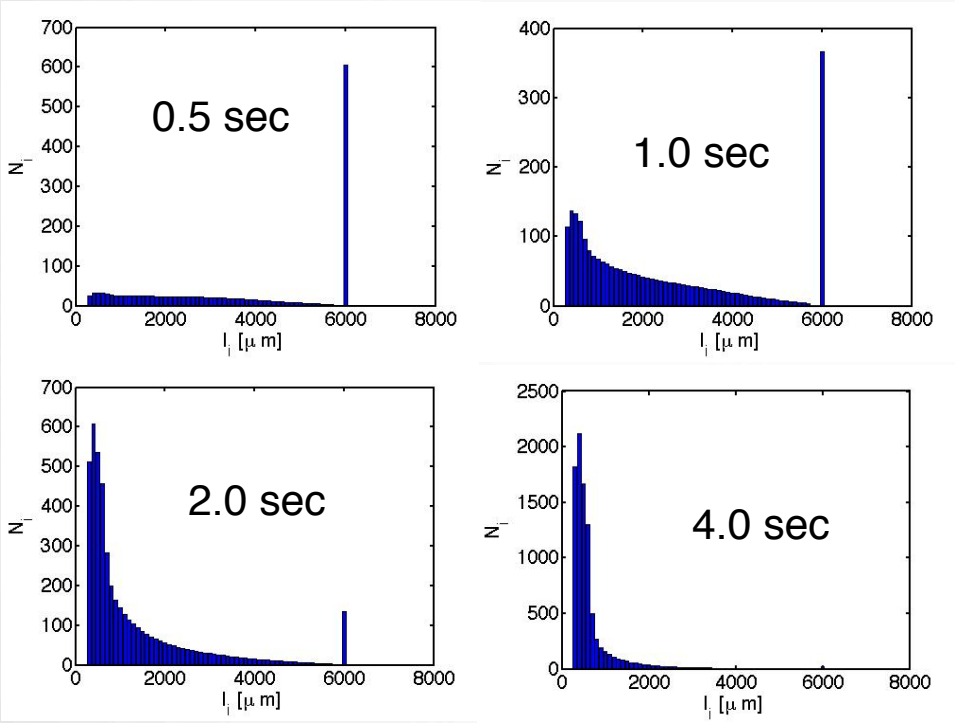

Conditions

IC: 1000 fibers
6 mm long

$\dot{\gamma} = 500\ \mathrm{s}^{-1}$

$\eta_m = 1000\ \mathrm{Pa} \cdot \mathrm{s}$

$E_f = 73\ \mathrm{GPa}$

$d_f = 17\ \mu\mathrm{m}$

Parameters

$\zeta = 3$

$C_B = 2 \times 10^{-3}$

$S = 0.25$

For mold filling, add advection term and solve for FLD at each node

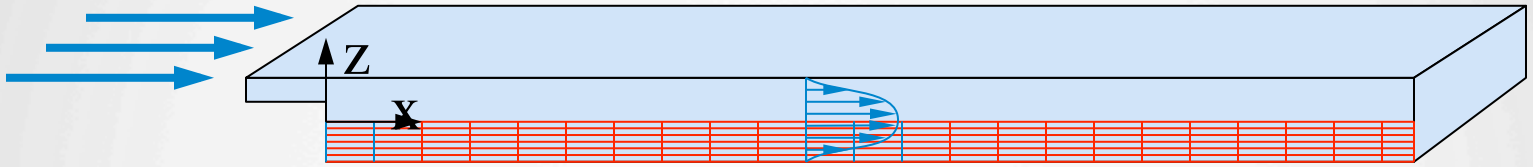

$$\frac{\partial N_i}{\partial t} + \mathbf{v} \cdot \nabla N_i = -P_i N_i + \sum_k R_{ik} N_k$$

- Currently 130 variables per node (!)
- Use experimental FLD just inside the gate as the initial condition
- Three adjustable parameters:

ζ (unbreakable length)

C_B (overall breakage rate)

S (child length distribution)

Numerical treatment of the fountain flow affects the fiber length predictions

physically

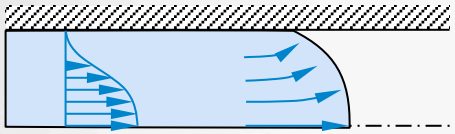

material deposited on the walls comes from the midplane

numerical treatment 1

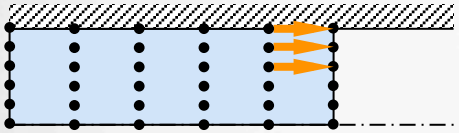

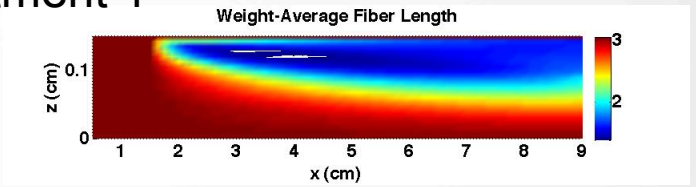

numerical treatment 2

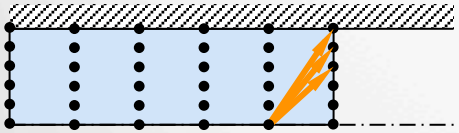

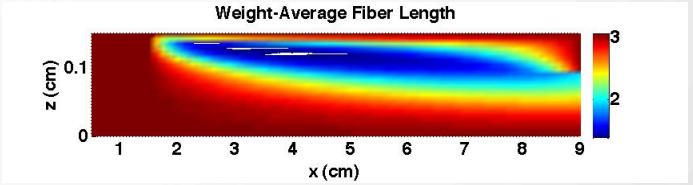

Predictions are a good match for through-thickness average length data

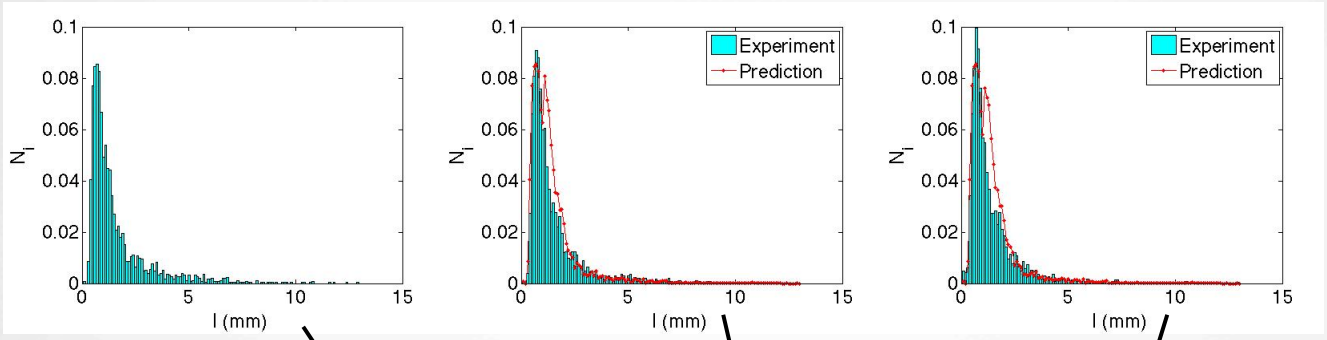

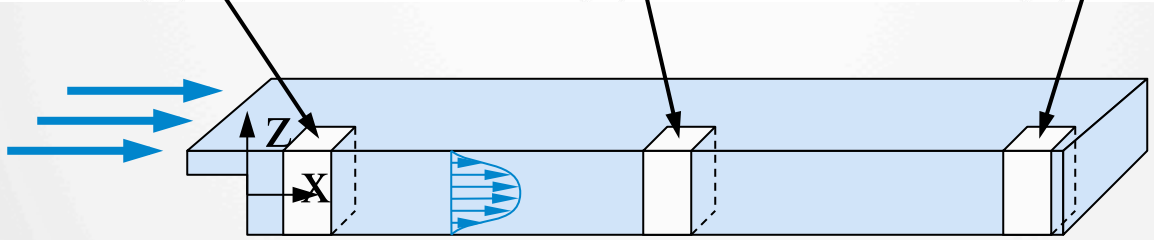

$\zeta = 0.55$ $C_B = 0.025$ $S = 1.0$

Average fiber lengths vary along the flow path and across the thickness

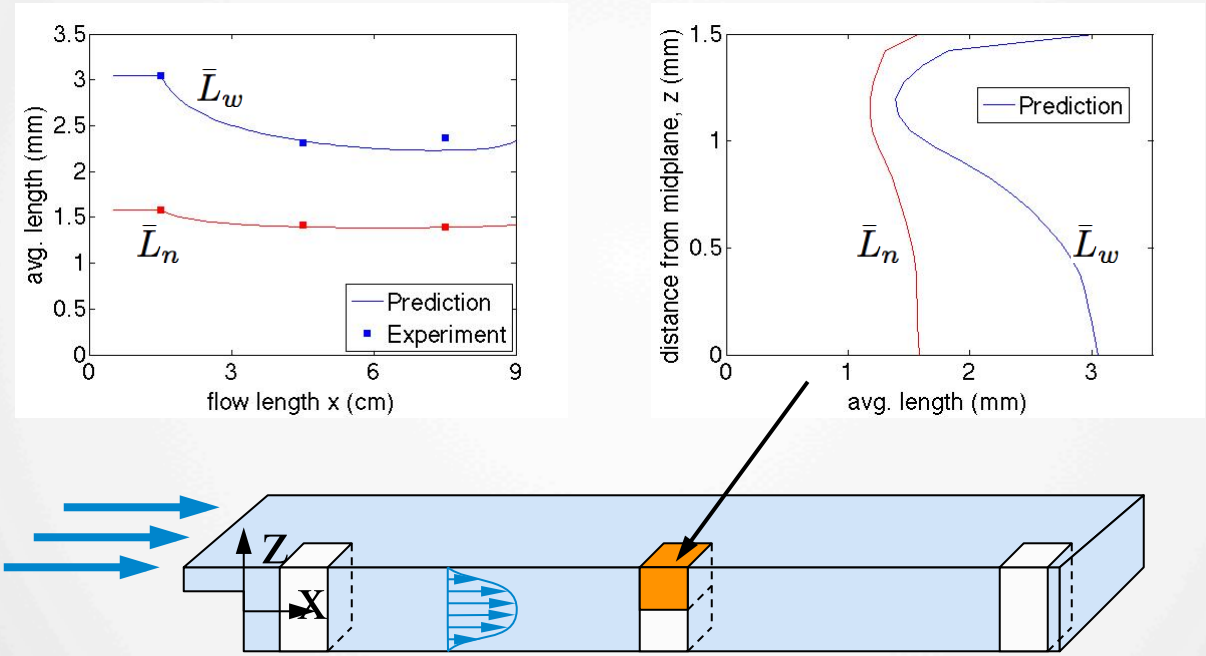

Predictions for a GF-PP center-gated disk (PNNL AF3D) are good

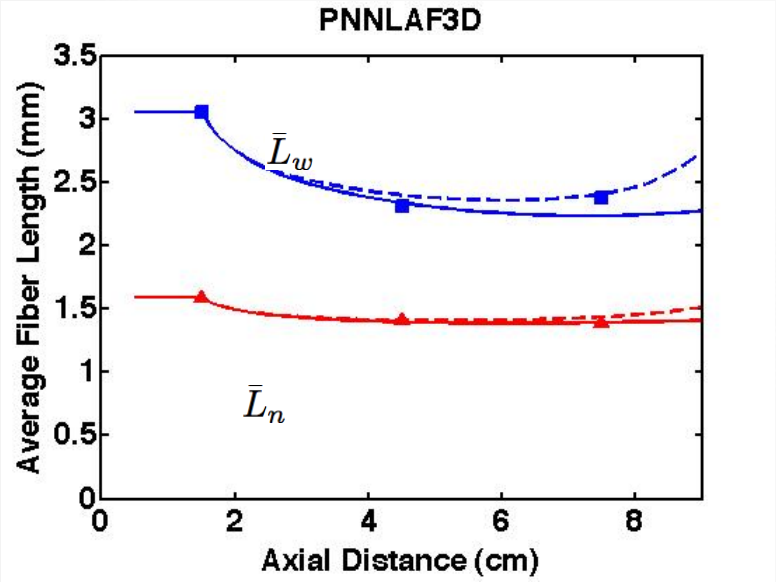

$\zeta = 0.55$

$C_B = 0.025$

$S = 1.0$

fountain 1

fountain 2

Fiber length generally decreases with flow distance, except for fountain effects

Conclusions, Fiber Length Model

- The model structure and preliminary results are useful
- Improvements are likely to come from better modeling of the breakage probability, P_i
  - include flow-type and orientation state dependence? (**D**, **A**)
  - better understand volume-fraction and length dependence
- Need to simplify or transform the model to speed up computation
  - 130 vars. per node = TOO MUCH COMPUTING!
  - Fiber orientation is routine, uses 5 variables/node

J. H. Phelps and C. L. Tucker, *Composites: Part A*, Vol. 51, pp 11-21, 2013.